Journal Pre-proof

Statistical relationships between large-scale circulation patterns and local-scale effects: NAO and rainfall regime in a key area of the Mediterranean basin

Marco Luppichini, Michele Barsanti, Roberto Giannecchini, Monica Bini

PII: S0169-8095(20)31207-2

DOI: https://doi.org/10.1016/j.atmosres.2020.105270

Reference: ATMOS 105270

To appear in: *Atmospheric Research*

Received date: 2 May 2020

Revised date: 11 September 2020

Accepted date: 17 September 2020

Please cite this article as: M. Luppichini, M. Barsanti, R. Giannecchini, et al., Statistical relationships between large-scale circulation patterns and local-scale effects: NAO and rainfall regime in a key area of the Mediterranean basin, *Atmospheric Research* (2020), https://doi.org/10.1016/j.atmosres.2020.105270

Statistical relationships between large-scale circulation patterns and local-scale effects: NAO and rainfall regime in a key area of the Mediterranean basin

Marco Luppichini[a,*], Michele Barsanti[b], Roberto Giannecchini[c], Monica Bini[c]

[a]Department of Earth Sciences, University of Study of Florence, Via La Pira 4, Florence, Italy.

[b]Department of Civil and Industrial Engineering, University of Pisa, Largo L. Lazzarino, 56122 Pisa, Italy

[c]Department of Earth Sciences, University of Pisa, Via S. Maria, 52, 56126 Pisa, Italy

Abstract

In this work, we investigated the correlation between the North Atlantic Oscillation (NAO) index and the rainfall trend in Tuscany (Italy) by using a large number of rain gauges for a high-resolution spatial scale study in a region characterized by significant morphological and climatic variability and equipped with an efficient measurement network. The relationship between NAO and rainfall was calculated by the Spearman's correlation coefficient. Our study shows that the correlation between NAO and precipitation has two types of oscillations as functions of the time scale. During the year the correlation is negative in winter and positive in summer, and this is due to global atmospheric circulation, which causes the area to be affected by humid air masses from the Atlantic Ocean during the winter. It is difficult to understand these experimental observations for the summer period because the correlation is influenced by the low rain levels of this area and the results could be easily influenced by other global patterns. Investigating in particular the period from December to March, we observed a variation in the NAO precipitation correlation also over time, with periods characterized by an increase in anti-correlation. The results obtained for Tuscany were contextualized and compared with other areas of Europe and of the Mediterranean basin by applying the same methodology. Spatial analysis showed that the trend of the NAO and rainfall correlation depends on latitude. In northern Europe, the behaviour of the correlation between NAO and rainfall over time is very similar to the temporal trend of NAO itself; instead, in the southern Mediterranean area this correlation has a trend over time that is very similar to the one of the Atlantic Multidecadal Oscillation (AMO) Index. This allowed us to observe a different regulation in the circulation of the humid air masses coming from the Atlantic Ocean, which induced rainfall in the Mediterranean and in northern Europe. The circulation of humid air masses in Northern Europe is linked to the pressure difference between high and low latitudes (represented by the NAO index), whereas in the Mediterranean it is linked to the temperature of the Atlantic Ocean (represented by the AMO index). The areas between high and low latitudes, characterized by a mixed behaviour, are regulated by both pressure difference and ocean temperature. This study has made it possible to investigate a specific area of the Mediterranean and then to extend and contextualize to more geographical locations, highlighting the fact that simple linear regression models can help to investigate the role of global patterns on the local effects.

Keywords:

NAO, AMO, rainfall, Spearman's correlation coefficient, climate patterns, Tuscany.

*Corresponding author.
Email addresses: marco.luppichini@unifi.it (Marco Luppichini), michele.barsanti@unipi.it (Michele Barsanti), roberto.giannecchini@unipi.it (Roberto Giannecchini), monica.bini@unipi.it (Monica Bini).

1. Introduction

Current global warming directly affects the different components of the hydrological cycle (Allan, 2011; Bates et al., 2008). Such components include precipitation and temperature patterns, frequency and intensity of extreme events, and changes in soil moisture (Stagl et al., 2014; Xu et al., 2011), with substantial consequences in terms of socio-economic conditions and financial policy of the countries involved. For instance, from 1980 to 2017 Germany, Italy, France and the United Kingdom are the European countries that spent the highest amount of money due to the impact of extreme weather and climate-related events (European Environment Agency, 2019). One of the main drivers of winter climatic variability in the Northern Hemisphere is the North Atlantic Oscillation (NAO; Hurrell, 1995; J.W. Hurrell, Y. Kushnir, G. Ottersen, 2003). NAO is a north-southern dipole of pressure anomalies, with a pole positioned at a higher latitude (Icelandic low) and the other at the central latitudes of the Northern Atlantic between 35°N and 40°N (Azores high). NAO influences climatic patterns in all seasons, but its influence is more evident during the winter months (Barnston and Livezey, 1987; Hurrell et al., 2003). In particular, the negative phases of the NAO winter are associated with wetter conditions in the Mediterranean basin and drier conditions in northern Europe, whereas the opposite occurs during the NAO positive phases (Osborn, 2006). For this reason, NAO is considered the dominant mode of regulation of winter climate variability in the Northern Atlantic area, in southern Europe and in the Mediterranean basin at a monthly-to-decadal timescale (Herrera et al., 2001). Many studies have investigated the influence of NAO on climatic patterns: changes in the surface westerlies across the Atlantic and Europe (van Loon and Rogers, 1978), precipitation (Folland et al., 1986; Hurrell, 1995a; Lamb and Peppler, 1987; Ulbrich et al., 1999; Zorita et al., 1992), changes in the Atlantic storm tracks and frequency (Hurrell, 1995b; Rogers, 1990), temperature (Hurrell, 1996; Moses et al., 1987; Parker and Folland, 1988; Van Loon and Williams, 1976), and sea surface salinity (Molinari et al., 1997; Reverdin et al., 1997). In particular, several studies have investigated NAO influence on the precipitation regime of various sectors of the Mediterranean basin, resulting in a strong influence in the Iberian Peninsula (Goodess and Jones, 2002; Muñoz-Díaz and Rodrigo, 2003; Ríos-Cornejo et al., 2015; Trigo et al., 2004), and largely influencing the rainfall amount in Italy (Brandimarte et al., 2011; Caloiero et al., 2011; Ferrari et al., 2013; Romano and Preziosi, 2013; Vergni et al., 2016). The study of forcing, which regulates the relationship between rainfall and NAO, is crucial to understand modern climatology at a regional scale, to reconstruct past evolution, and to forecast future scenarios. As demonstrated by Vicente-Serrano and López-Moreno (2008), the relationship between NAO and rainfall has not been constant over time. Since the beginning of the 1900s until now, periods characterized by a stronger relationship between NAO and precipitation have been alternated with periods exhibiting an opposite behaviour. In Europe, this trend also shows a very complex spatial variability, which depends on global factors (e.g. baric dipole positioning, intensity of baric difference, etc.) and on local factors (e.g. morphology of the territory). NAO varies over time not only in terms of intensity but also in terms of position of the pressure differential. The position of the baric dipole influences the European climate. Generally, NAO models moved eastward induce a stronger than average influence on European temperature. In contrast, the effects of NAO on European rainfall anomalies are less consistent, with a different response from each area. Not only the temporal but also the spatial variability of NAO is important in regulating the European climate (Luo et al., 2018). There is also a strong asymmetry of the NAO between its two phases in amplitude, persistence and zonal movement. The negative NAO phases are characterized by large amplitude, by a westward movement and by longer persistence. Opposite features are observed for positive NAO (Rousi et al., 2020) .

The aim of this work was to explore effective statistical approaches in order to highlight the correlation between NAO and rainfall amount at a regional scale. The correlation between pressure difference (NAO) and rainfall could be linked to the temperature of the Atlantic Ocean, which is a potential vector regulating both variables. Therefore, in our

analyses we introduced Atlantic Multidecadal Oscillation (AMO), a low frequency large-scale mode of Sea Surface Temperature (SST) variability in the North Atlantic. This oscillating oceanic phenomenon is typically quantified by a spatially-weighted mean SST of the North Atlantic (0°-65°N), commonly referred to the AMO index. AMO exhibits a phase-switching (warming/cooling) behaviour with a periodicity of 60-80 years (Knight et al., 2006, 2005). For this study we selected the Tuscany Region (NW Italy) for different reasons, in particular for the availability of more than 300 rain gauges, most of them yielding data since the beginning of the last century. The advantages of studying this region are also related to its peculiar position within the Mediterranean basin, since its climatology depends on the air masses of Atlantic origin, which are perturbations linked to Mediterranean circulation and to the inclusion of cold air masses coming from northern Europe. Moreover, its heterogeneous morphology involves different microclimates in several sectors connected to local factors such as orographic effects (Geiger et al., 1995). A linear model describing the relationship between NAO and rainfall is also proposed for Tuscany and Europe.

2. Materials and Methods

2.1. Study area

Located in central Italy, Tuscany is 22,985 km^2 wide (**Error! Reference source not found.**). Its western border is represented by the sea (Ligurian Sea in the north, Tyrrhenian Sea in the south). The Tuscan morphology is characterized by several alluvial plains located mainly in the central part of the region, whereas mountains with a different altitude (up to more than 2,000 m) are mainly located in the northern and eastern sectors (**Error! Reference source not found.**). The main rainy season is autumn, with a progressive decrease generally starting in December (**Error! Reference source not found.**). Mean annual precipitation (MAP) is influenced by the topography of the area and is linked to altitude (Figure 3b). The rainiest areas are located at the highest altitude (Apuan Alps and Apennines). In particular, the Apuan Alps, in northwestern Tuscany, show some of the highest precipitation amounts in Italy (Giannecchini and D'Amato Avanzi, 2012; Rapetti and Vittorini, 1994), often characterized by high intensity (D'Amato Avanzi et al., 2004; Giannecchini, 2006).

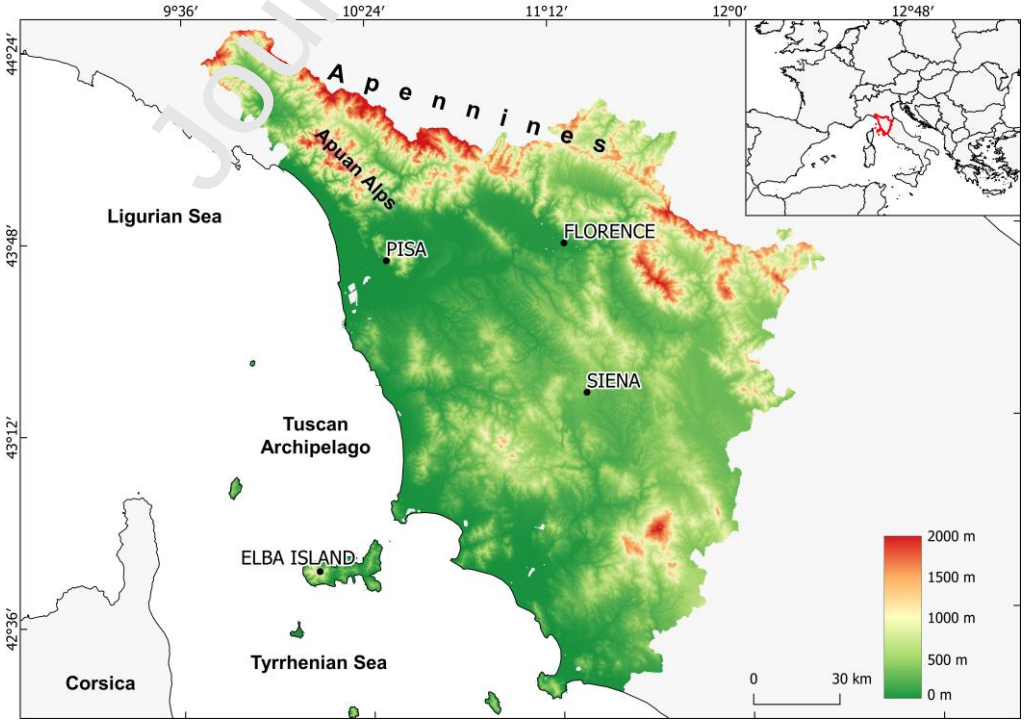

Figure 1: Tuscany Region (10x10m DTM resolution provided by the Tuscany Regional Service).

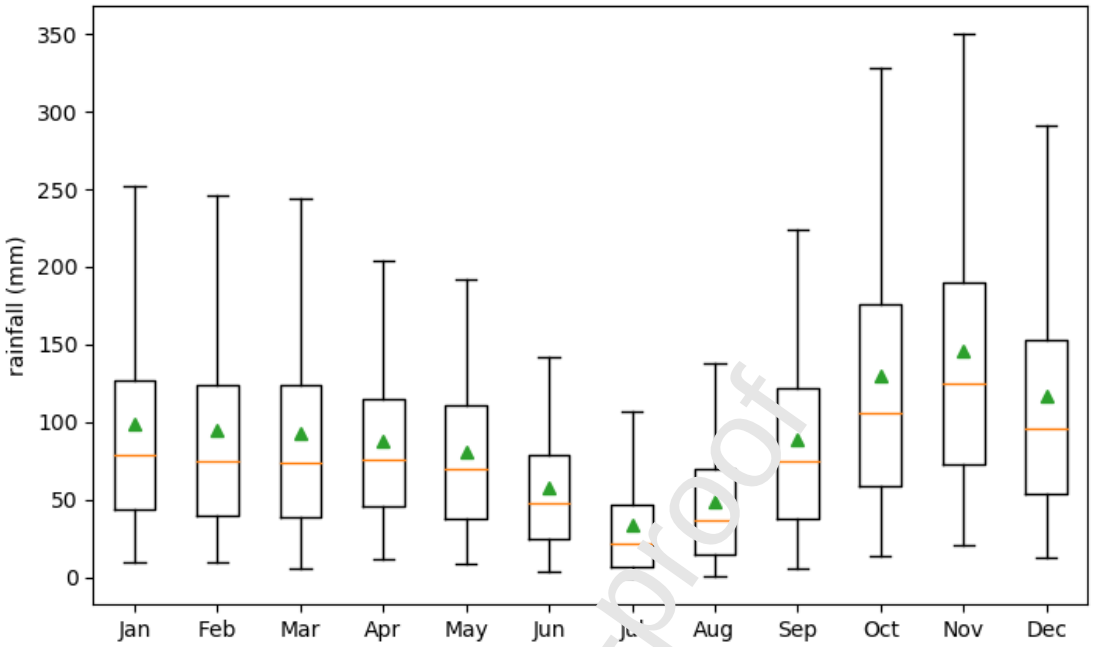

Figure 2: Mean seasonal rainfall distribution in Tuscany obtained from the 1075 rain gauges of Figure 3a. The orange lines represent the median, the whiskers represent the 5th and 95th percentiles, the boxes represent the 25th and 75th percentiles, and the green triangle represents the mean.

2.2. Databases

In this work we used various types of data from different sources. The different databases and the preliminary data processing are described in the following sections.

2.2.1. Rainfall dataset

The rain-gauge dataset was provided by the Tuscany Region Hydrologic Service Network and includes 1075 stations not evenly distributed over the territory (Figure 3a and 3c), the density being commonly higher in the mountain areas. The data was obtained by an automated download procedure through codes written in Python and through the HTTP protocol. The older stations have started monitoring since the beginning of the last century, even if temporal continuity of the data is not always guaranteed for all the stations. From 1935 to date, approximately 300 rain gauges have been active every year (Figure 4). The Regional Hydrological Service provides the daily rainfall data for each rain gauge in the operation period. The total number of datapoints used in this work is slightly exceeds 10 million: about 89% is validated by the Regional Hydrological Service, about 10% is pre-validated by the Regional Hydrological Service and about 1% is missing data. Pre-validation is a methodology applied by the Regional Hydrological Service to analyze the new data and to simplify the validation procedure. The pre-validation procedures can evidence macro errors such as instrument malfunction or missing data.

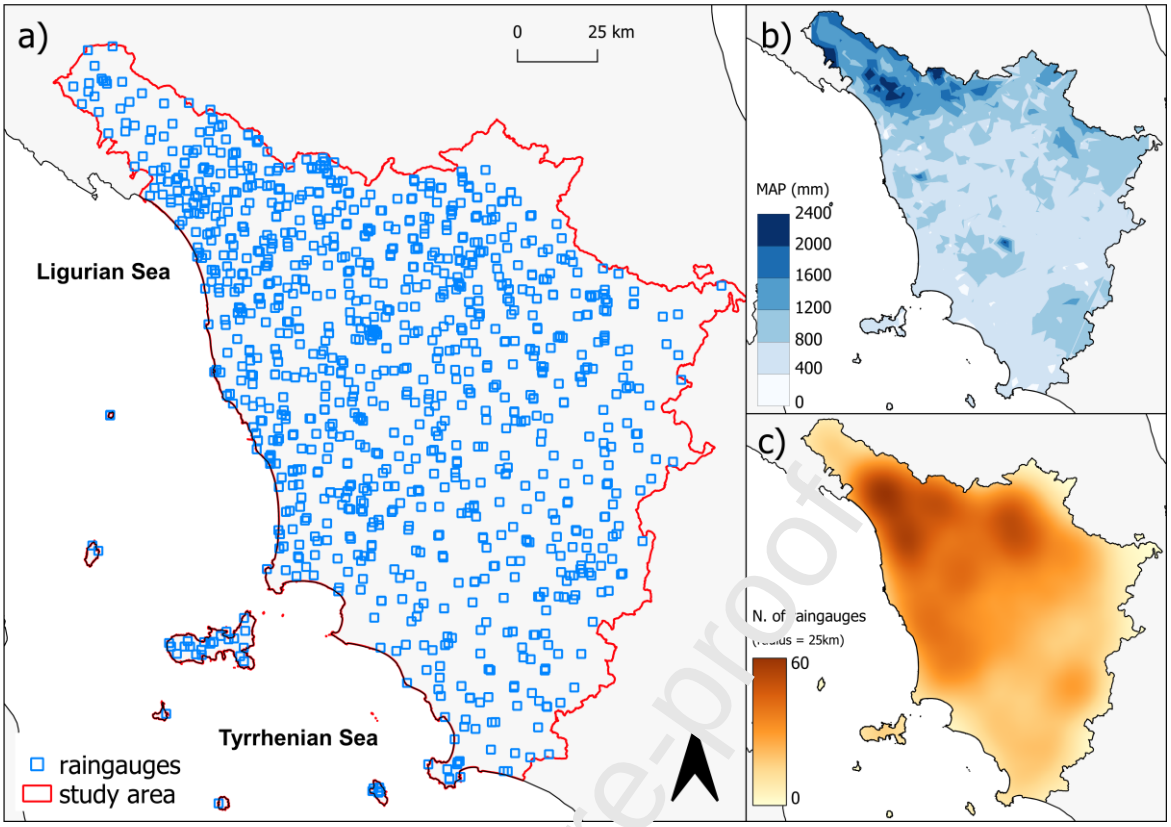

Figure 3: a) rain-gauges of the Regional Hydrologic Service Network; b) mean annual precipitation calculated by using 1075 rain gauges; c) heatmap of the number of rain-gauges with 25 km radius setting.

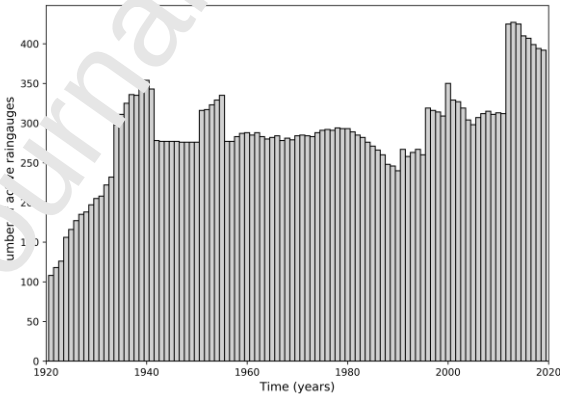

Figure 4: Number of yearly active rain gauges from 1920 to date.

2.2.2. North Atlantic Oscillation (NAO) dataset

The NAO dataset used in this paper is provided by the Climate Analysis Section of the US National Center for Atmospheric Research (NCAR). This dataset is based on the differences of normalized sea-level pressure (SLP) between Lisbon (Portugal) and Stykkisholmur/Reykjavik (Iceland) since 1864. The SLP values at such stations were normalized by removing the long-term mean and dividing the resulting value by the long-term standard deviation. Both long-term mean and standard deviation are based on the 1864-1983 period. The data provided were normalized so as to avoid that the series could be dominated by the greater variability of the northern station (Hurrell and National Center for Atmospheric Research Staff, 2020).

2.2.3. *Atlantic Multidecadal Oscillation (AMO) dataset*

The Atlantic Multidecadal Oscillation (AMO) highlights the multidecadal variations in Atlantic Sea Surface Temperatures (SSTs) between the Equator and Greenland (Knight et al., 2005). AMO is one of the main climatic indices used to describe the regulation of rainfall in Europe, especially in the northwestern area. The time-series, available since 1856, is calculated from the Kaplan SST dataset (https://psl.noaa.gov/data/gridded/data.kaplan_sst.html), which is updated on a monthly basis. The dataset employed in this work is provided by the Earth System Research Laboratory (ESRL) of the NOAA Institute (https://www.esrl.noaa.gov/psd/data/timeseries/AMO/).

2.3. *Data processing*

Two different approaches were used to correlate climate index and rainfall data. In the first case, the statistical procedure was applied by grouping the data of each rain gauge to obtain the monthly cumulated rainfall over the entire period. In the second case, only the data acquired from December to March (December-January-February-March, DJFM) have been used in the period from 1920 until today. Since it is not necessary in this study to completely exclude time-series with missing values, a precautionary analysis methodology was used to achieve the monthly cumulated rainfall data from the grouping of the daily data. The criterion we used was based on the typical characteristics of the data available. Most of the time-series had gaps of less than one week a month. On this basis, in our study we discarded the months during which daily-cumulated rainfall recordings had been missing for over 20% of days. For correlation coefficient calculation, we did not need the time series to be continuous; therefore, we discarded only that data, keeping as much valid data as possible. To neglect any effects of an excessively small time-scale in the development of the linear model, the NAO and AMO data were smoothed over a 30-year moving window.

In the development of the model, the average value of NAO and AMO was subtracted from both indices, and both were made dimensionless by dividing the zero-mean time-series by their standard deviations, so that NAO and AMO could be compared with a correlation coefficient (whose dimensionless values range between −1 and 1). Even if this standardization does not affect the computation of the correlation coefficient, it is useful if one wants to explain a correlation coefficient (dimensionless) in terms of NAO and AMO values, which are usually reported in physical units.

2.4. *Statistical procedure*

2.4.1. *Dickey-Fuller test*

The Dickey-Fuller (DF) statistical test (Dickey and Fuller, 1979) is useful to determine whether a time interval of duration such as the NAO time-series can be considered stationary from a statistical point of view. In this test, the null-hypothesis H_0 includes two conditions: i) the investigated time-series is non-stationary; ii) the time-series can be described using either an autoregressive (AR) process of an order ≥1 or, in a more general approach, using a moving average autoregressive process ARMA (p,q), where p and q indicate the orders of the autoregressive and moving average components. In this case, the stationarity test is called Augmented DF Test (ADF). H_0 is verified by checking whether the characteristic time-series polynomial obtained from an AR or ARMA model has a unit root. The ADF test was performed using the Python open-source statsmodels library, in particular the adfuller method. The test result is evaluated by analyzing the p−value: if its value exceeds a critical threshold (usually set to 0.05), H_0 cannot be rejected; if the p-value is ≤0.05, H_0 is rejected, and the time-series can be considered stationary. This means that no trend is present. The stationarity hypothesis is important when a comparison is performed between several time series. A correlation can be inferred when changes are detected in the values of different time series. For this correlation to be

significant, all the considered time series must be stationary. To identify the minimum duration of the time window in which the NAO time-series can be considered stationary, we conducted an ADF test using moving windows lasting between 2 and 50 years. The test showed that the NAO series can be considered stationary over time intervals higher than 10 years. In agreement with the climatological normal (WMO, 2007) and other studies (such as Vicente-Serrano and López-Moreno, 2008), we chose time windows of 30 years. Thus, we used rain gauges with a time-series longer than 30 years and set up a 30-year mobile window to analyze variability over time. The total number of rain gauges selected was 369 (Figure 5).

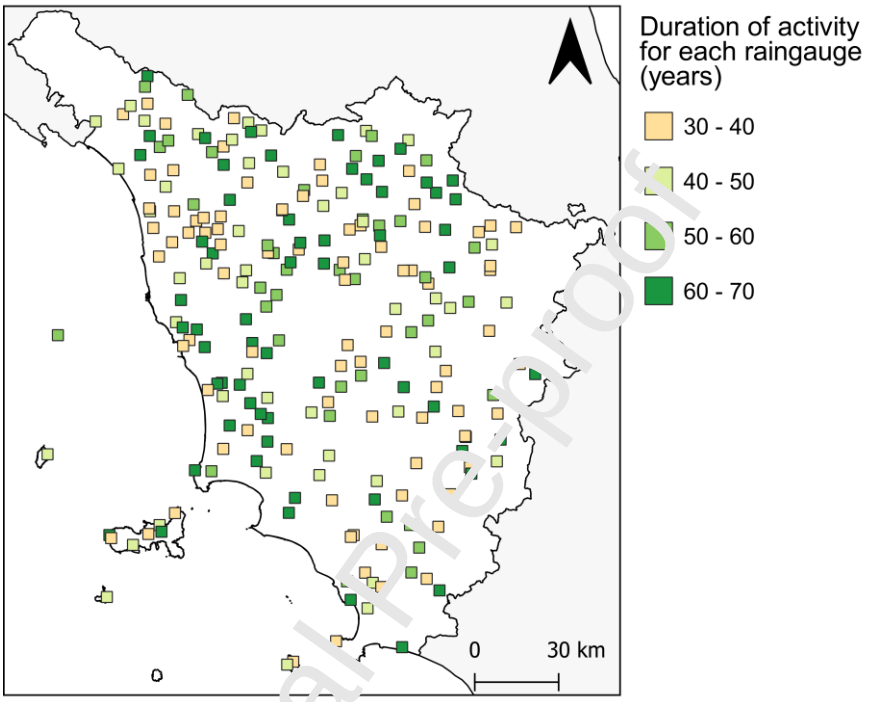

Figure 5: Rain gauges used in this study. The colors represent the different duration of activity for each rain gauge. In this work, we used only the rain gauges with a duration of activity greater than 30 years.

2.4.2. Statistical correlations

We calculated the correlation coefficient to identify a possible relationship between NAO and rainfall amount. Some authors (Brandimarte et al., 2011; Faust et al., 2016; Kalimeris et al., 2017; Kotsias et al., 2020; Koyama and Stroeve, 2019; López-Moreno et al., 2011; Vicente-Serrano and López-Moreno, 2008) use Pearson's correlation coefficient, a measure of the linear association between two variables. To quantify the relationship between NAO and rainfall (Caloiero et al., 2011; Izquierdo et al., 2014; Nalley et al., 2019; Vergni et al., 2016) other authors use Spearman's correlation coefficient (SCC) (Spearman, 1904), which is suitable for monotonically-related variables, even when their relationship is not linear.. The range of both Pearson's and Spearman's coefficients is [-1,+1]; positive values indicate a tendency of one variable to increase or decrease together with another variable, whereas negative values indicate a trend in which the increase in the values of one variable is associated with the decrease in the values of the other variable, and vice versa. The Q-Q plot of the NAO data (Figure 6a) and the NAO empirical distribution (Figure 6b) qualitatively highlight that the distribution of NAO values is not normal; this is quantitatively confirmed by Shapiro's Test. Considering that rainfall distribution is not normal either, the use of Pearson correlation may lead to bias due either to skewed or heavy-tailed distributions, inflating the estimations of the correlation coefficients. In (Bishara and Hittner, 2015) is shown that Spearman correlation eliminates this inflation and provides estimates with a mean bias of -0.01.

Spearman coefficient has been successfully applied in (Qian et al., 2015) to show spatial correlation between SST anomalies and atmospheric circulation anomalies. The choice of Spearman correlation coefficient is therefore justified.

To investigate the trend, we calculated the SCC between NAO and the December–March (DJFM) precipitation values over a 30-year moving time-window. The first calculation used the data spanning over the first 30 years (1920-1950), and the result was assigned to the year halfway through this period (1935). The time-window was then shifted by one year, and the data from 1921 to 1951 were used for the calculation, assigning the result to the year 1936. This process was repeated until the time window reached the years 1990-2020.

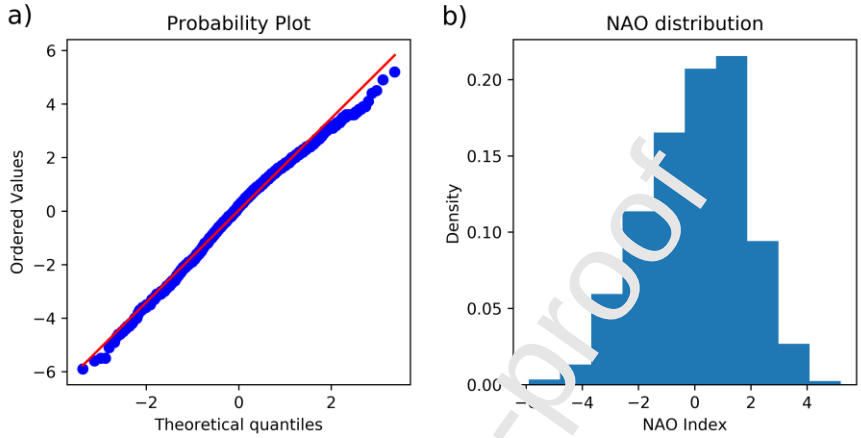

Figure 6: Statistical distribution of NAO time-series: a) quantile-quantile (Q-Q) plot of the NAO time-series, b) histograms with 10 bins of NAO time-series.

3. Results and Discussion

3.1. Correlation of NAO and rainfall throughout the region

Figures 7, 8 and 9 show the results of the SCC calculation and the SCC changes during the year. February and June show the highest values of anti-correlation and correlation, respectively. The highest spatial variability occurs in spring and autumn. In June and July, the entire area is generally characterized by a positive correlation, but the correlation is negative from December to March (DJFM). In the remaining months of the year, the correlation does not show a clear distribution in the different zones. The seasonal and spatial variation of SCC is in general agreement with other studies in Italy (Caloiero et al., 2011; López-Moreno et al., 2011; Vergni et al., 2016; Vicente-Serrano and López-Moreno, 2008). There is a pronounced negative correlation in winter and a positive correlation in summer, whereas spring and autumn are characterized by the highest spatial variability (Figure 7). The use of a high density network of rain gauges made it possible to characterize the climatic zones of Tuscany in more detail. The months from October to December clearly show the transition of the polar front between summer and winter. In fact, in October there is no correlation between NAO and rainfall in northern Tuscany, while the southern area has a positive correlation. In November, there is a more negative correlation in the northern area, while there is no correlation in the southern area. In December the whole area shows a negative correlation. Therefore, in these months a progressive anti-correlation increase can be observed from north to south. In June, the lowest correlation values are found near the main mountain ranges in Tuscany. This is particularly visible in northern Tuscany, where the Apuan Alps and the Northern Apennines are located. In June, when the polar front is stationed at high latitude, moist air masses can occasionally be directed towards the Mediterranean basin. These air mass incursions and their impact on the mountains generate local climatic instability, producing an anti-correlation between rainfall and NAO in this area. However, the general climatic stability caused by the High Azores creates a positive correlation between rainfall and NAO in the rest of the region. Figure 8 shows the

percentage error of Spearman's correlation coefficient (Bowley, 1928) for all months. In this area the quality of the dataset is not homogeneous because some areas are represented by a higher number of data with respect to others.

In the months when the percentage error is generally low, the results can be considered more reliable. In the area, the minimum percentage error values are recorded in the months from December to March. This valuation of the errors of SCC confirms our choice of wanting to investigate in greater detail only the months from December to March which results are certainly more reliable and the correlations (or anti-correlations) between NAO and rains are greater.

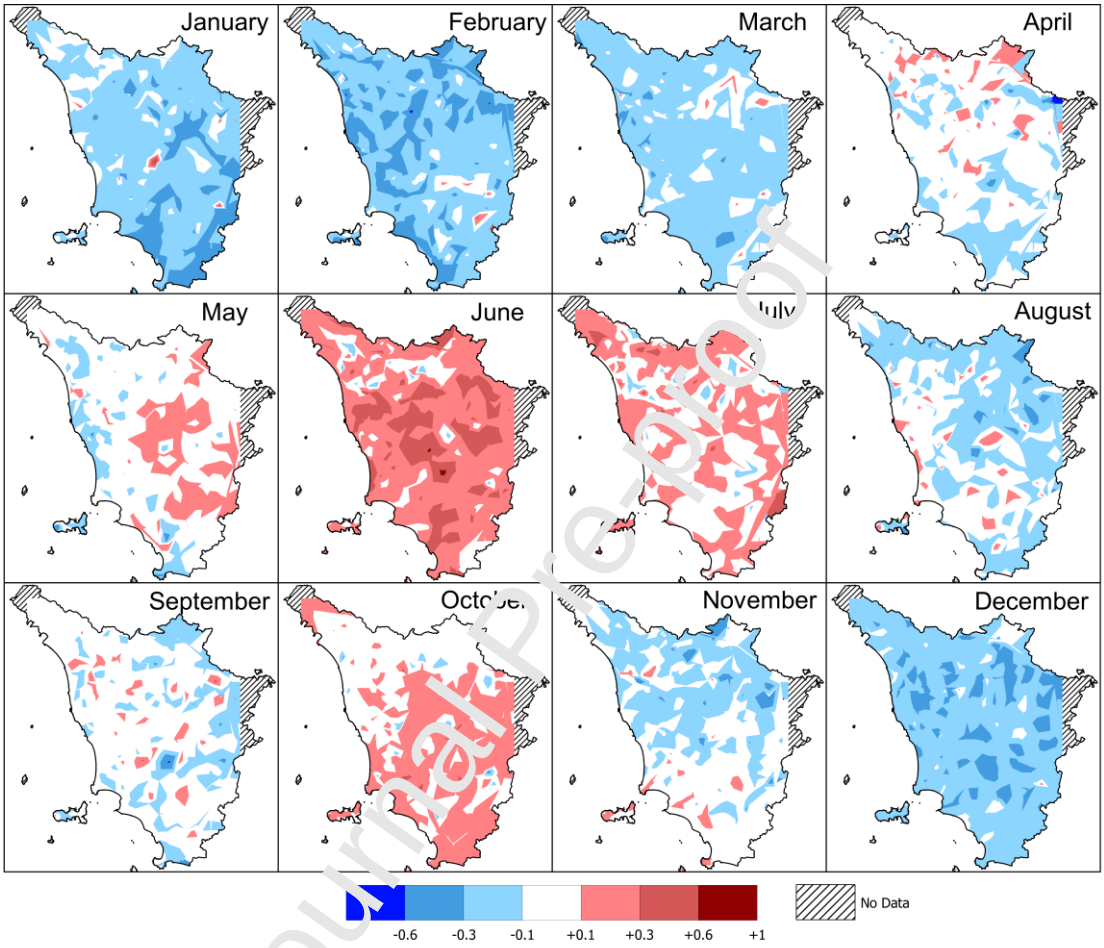

Figure 7: Spatial distribution of Spearman's coefficient of correlation between the NAO dataset and the monthly rainfall in Tuscany (results obtained using rain gauges with a period of activity higher than 30 years; rainfall and NAO datasets from 1920 to 2019).

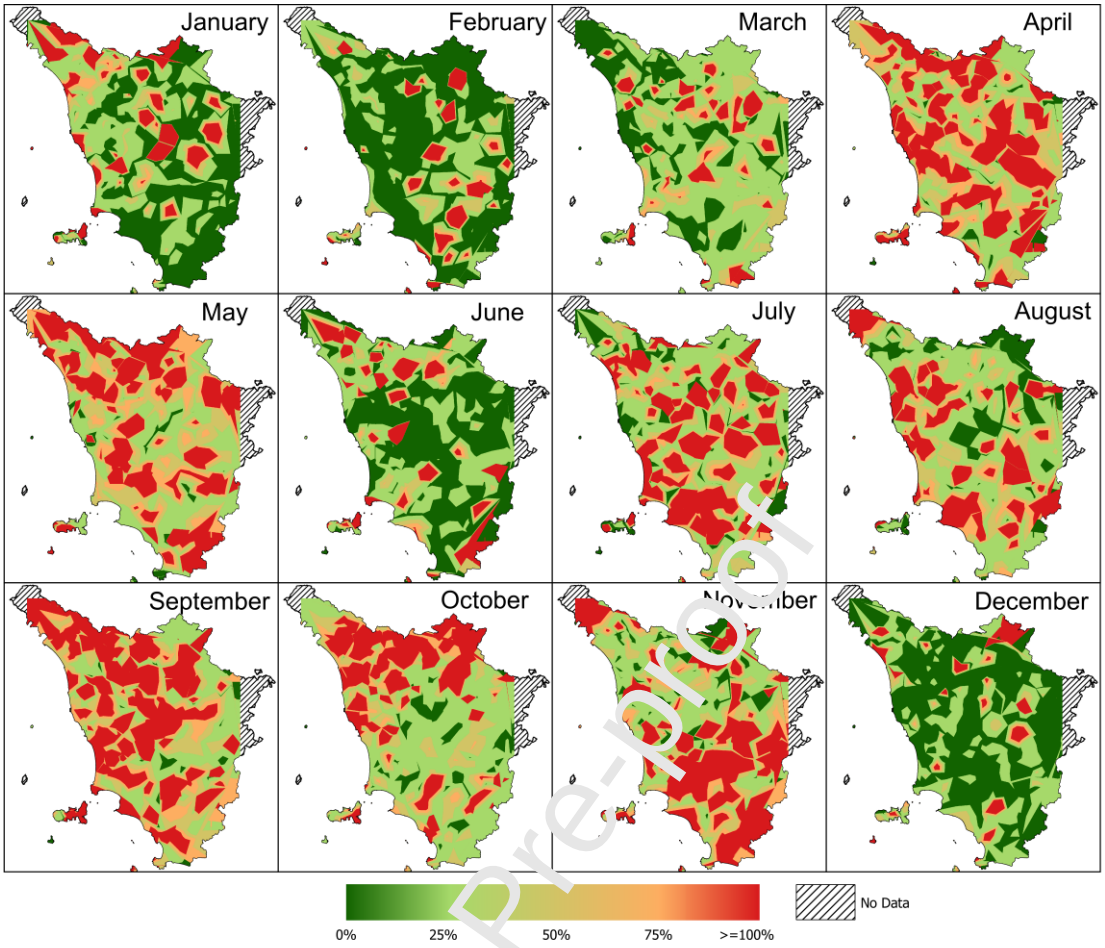

Figure 8: Spatial distribution of percentage error of Spearman's coefficient of correlation between NAO dataset and monthly rainfall in Tuscany.

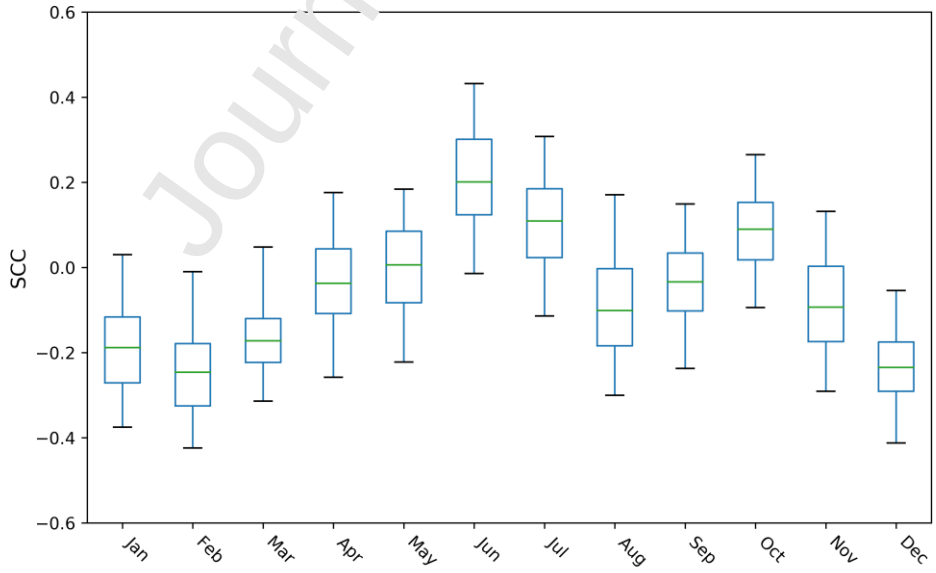

Figure 9: Statistics of Spearman's correlation coefficient between NAO dataset and monthly rainfall in Tuscany (elaboration obtained using rain gauges with a period of activity higher than 30 years; rainfall and NAO datasets from 1920 to 2019). The green line represents the median, the whiskers represent the 5th and 95th percentiles, and the box represents the 25th and 75th percentiles.

3.2. *Correlation of NAO and rainfall over time*

Figure 10 shows the variation of SCC for DJFM rainfall over time. The blue band represents the standard deviation. Over time, the SCC curve shows a minimum in the correlation value between the 60s and 90s of the past century. There is a progressive decrease and increase in the correlation before and after this period.

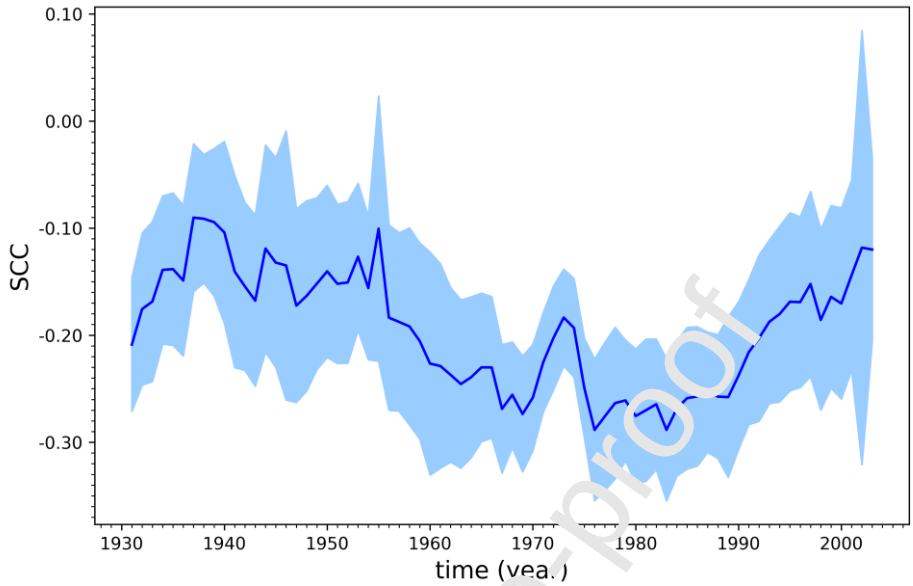

Figure 10: Spearman's coefficient of correlation (SCC) over time calculated on the December-March (DJFM) North Atlantic Oscillation data and rainfall dataset. The blue band represents the standard deviation.

The data available indicate that the correlation between NAO and rainfall has varied over time, in agreement with Vicente-Serrano and Lopez-Moreno (2008). Figure 10 shows the changes in time of the SCC over thirty-year mobile windows. The area was characterized by a decrease in SCC between 1960 and 1990, followed by a progressive increase until today. The trend of the correlation between SCC and rainfall is particularly complex. We tried to explore the possible effects of DJFM AMO in controlling changes in the correlation between NAO and rainfall, in order to explain the fluctuations of the DJFM SCC curve. In Figure 11 we compare the relation between the SCC curves and the AMO data averaged on a thirty-year mobile window. The SCC curve has a good correlation with DJFM AMO data and the trends are very similar. This observation indicates a possible influence of the temperature of the North Atlantic Ocean (represented by the AMO index) on the correlation between NAO and rainfall in Tuscany.

To quantify the influence of NAO and AMO on the SCC curve, we used a linear regression model (1) with the aim of finding the α and β parameters as weights of these two indices. We identified α, β and γ using an algorithm that minimized the sum of the quadratic deviations (2). The minimum was determined by imposing the constraint that α and β assume non-negative values, since we wanted to highlight the influence of the parameter (positive sign) and not the anti-influence of the parameter (negative sign). Anti-influence could be linked to other factors that the model does not take into consideration.

$$SCC = \alpha \cdot NAO + \beta \cdot AMO + \gamma \tag{1}$$

$$\sum_{i=0}^{n} (\alpha \cdot NAO_i + \beta \cdot AMO_i + \gamma - SCC_i)^2 = minimum \tag{2}$$

For the SCC curve, parameters α, β and γ were 0.0200, 0.0549, and −0.2006 respectively (Table 1). This indicates that for Tuscany the role of AMO in regulating SCC was greater than the influence of NAO during the December-

March period. In other words, at this time of year the SCC curve is by 70% influenced by SST and only by an approximate 30% by the pressure difference between two dipoles positioned at high and low latitudes. The model well approximates the SCC trend, as shown in Figure 11. In Tuscany the temperature of the Atlantic Ocean has a strong influence on the regulation of precipitations and of their origins. The influence of AMO on the correlation between NAO and rainfall could be related to latitude and, to confirm this observation, we used a grid-based rainfall database at a latitude/longitude resolution of 10' for all Europe (as compiled by the Climate Research Unit of the University of East Anglia, (http://www.cru.uea.ac.uk/timm/grid/TYNSC10.html). We applied our methodology to replicate part of the study by Vicente-Serrano and Lopez-Moreno (2008). Figure 12 shows the results obtained comparing the SCC, DJFM NAO, and DJFM AMO trends smoothed by using a 30-year moving window. The SCC curves at high latitudes (Edinburgh) have a completely different trend when compared with the curves at lower latitudes (Cairo). In the period from December to March a the role of NAO at high latitudes is crucial to explain the results of the correlation between NAO itself and rainfall. On the contrary, the SCC trend is determined by the DJFM AMO trend at lower latitudes. Table 1 shows the results of the linear model (1) for different latitudes. The values of the parameters obtained for Tuscany and Florence are very similar, and for this reason we can compare and validate the use of different types of data sets by observing that the linear model reasonably provides similar results. During the period December to March, when the pressure at lower latitudes is greater than at higher latitudes (negative NAO phase), the moist air masses coming from the ocean are directed towards the Mediterranean basin. During this phase, the correlation between NAO and precipitations at higher latitudes is zero (see the 1940-1960 period of Edinburgh in Figure 12). During the period from December to March, when the NAO is positive, the moist air masses are directed towards Northern Europe and we can observe an increase in the correlation between NAO and precipitation. Moving southwards, we observe a progressive loss of dependence of the SCC on the NAO trend. The greatest evidence of this loss of correlation can be observed at Cairo, where the relationship between DJFM NAO and DJFM rainfall is almost completely ruled by DJFM AMO, and secondly by SST. A high surface temperature of the Atlantic Ocean can be associated with a decrease in average pressure. In this case, the moist air masses can cause more intense rainfall in the drier areas of the Mediterranean basin. Finally, we can observe a progressive change from NAO to AMO regulation between high and low latitudes. Even if the linear model portends a certain global behaviour, we must also observe that in its simplicity it records the maximum errors in the phases of transition from one type of regulation to another. Passing from a linear model to a quadratic model the situation in some cases provides a better agreement, as we can observe in Figure 13. In this case, in addition to having a contribution from NAO and AMO, we also have a contribution from AMO^2, NAO^2 and from the product NAO · AMO. For Warsaw the Residual Standard Error (RSE) decreases from 0.085 to 0.072, for Wien the RSE decreases from 0.14 to 0.091 The use of a quadratic model in Northern Europe and in the Southern Mediterranean area does not actually improve the results. Moreover, using a more elaborate model it is more complicated to interpret the results and to explain the contribution of the various terms of NAO and AMO indices (linear, quadratic, crossed) on SCC. For this reason, we present here the results obtained with the simpler model, leaving the interpretation of results obtained using more complicated models to future developments of this work.

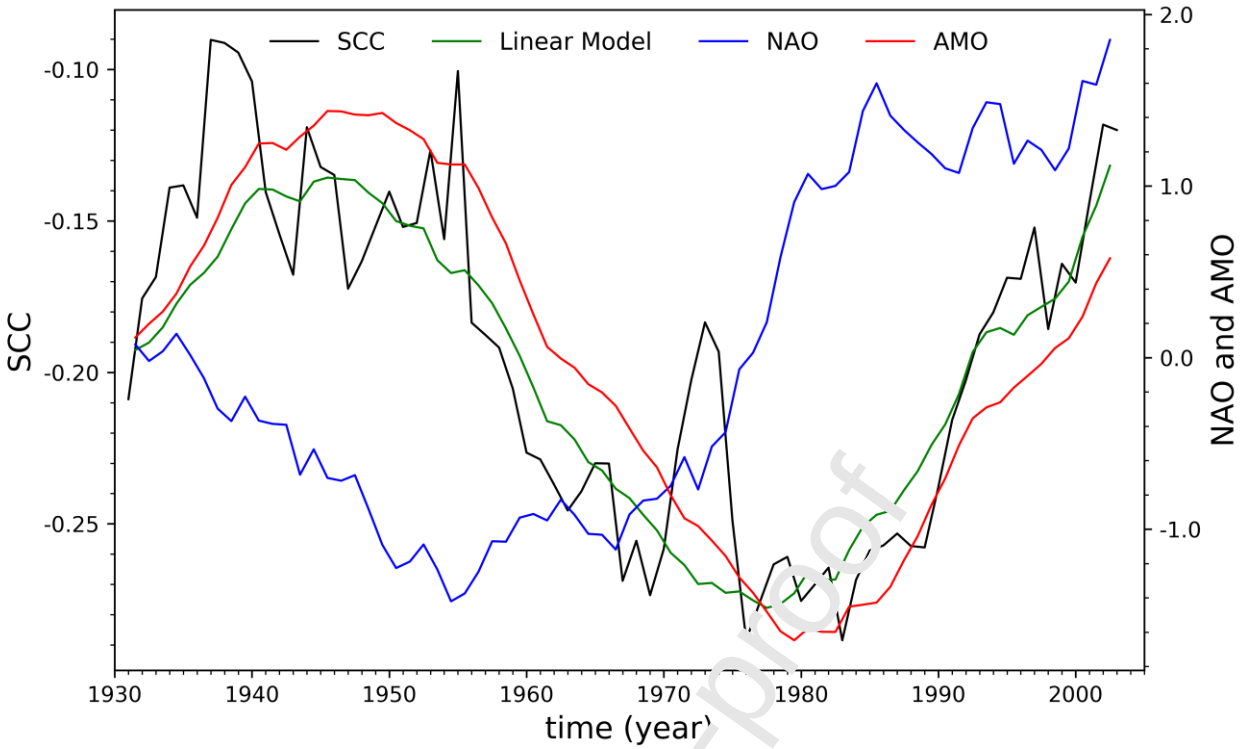

Figure 11: Spearman's correlation coefficient (SCC) between December and March (DJFM) North Atlantic Oscillation (NAO) and DJFM rainfall in Tuscany calculated on a 30-year mobile window (black line); DJFM NAO dataset averaged on a 30-year mobile window (blue line) and DJFM Atlantic Multidecadal Oscillation (AMO) averaged on a 30-year mobile window (red line); best-fit curve of the linear model (green line).

Location	Latitude	Longitude	α	β	γ	α%	β%	RSE
Tuscany	43.78*	11.24*	0.0200 ±0.0038	0.0549 ±0.0039	-0.2006 ±0.0034	27	73	0.029
Edinburgh	55.95	-3.19	0.203 ±0.021	0.0024 ±0.0206	0.304 ±0.017	99	1	0.16
London	51.51	-0.09	0.155 ±0.011	0	-0.018 ±0.011	100	0	0.10
Paris	48.85	2.34	0.195 ±0.015	0	-0.111 ±0.015	100	0	0.14
Warsaw	52.22	21.01	0.136 ±0.011	0.040 ±0.011	-0.0896 ±0.0090	77	23	0.085
Munich	48.13	11.57	0.1092 ±0.0091	0	-0.1332 ±0.0091	100	0	0.085
Wien	48.20	16.37	0.052 ±0.018	0.093 ±0.018	-0.114 ±0.015	36	64	0.14
Florence	43.78	11.24	0.027 ±0.015	0.050 ±0.015	-0.365 ±0.012	35	65	0.12
Bucarest	44.43	26.10	0.064 ±0.010	0.0026 ±0.0105	-0.3229 ±0.0085	96	4	0.080
Valencia	39.46	-0.37	0	0.086	-0.132	0	100	0.12

				±0.013	±0.013			
Athens	37.97	23.71	0	0.089 ±0.020	-0.020 ±0.019	0	100	0.18
Nicosia	33.36	35.17	0	0.208 ±0.026	0.052 ±0.025	0	100	0.24
Cairo	31.24	30.06	0	0.1549 ±0.0099	0.1010 ±0.0099	0	100	0.093

Table 1: α, β, γ values with their standard errors for the best-fit linear model *in different sites (α% and β% indicate each relative weight; RSE is the Residual Standard Error, which is a measurement of the lack-of-fit of the model). * For simplicity reasons, we associated the coordinates of Tuscany with those of the city of Florence.*

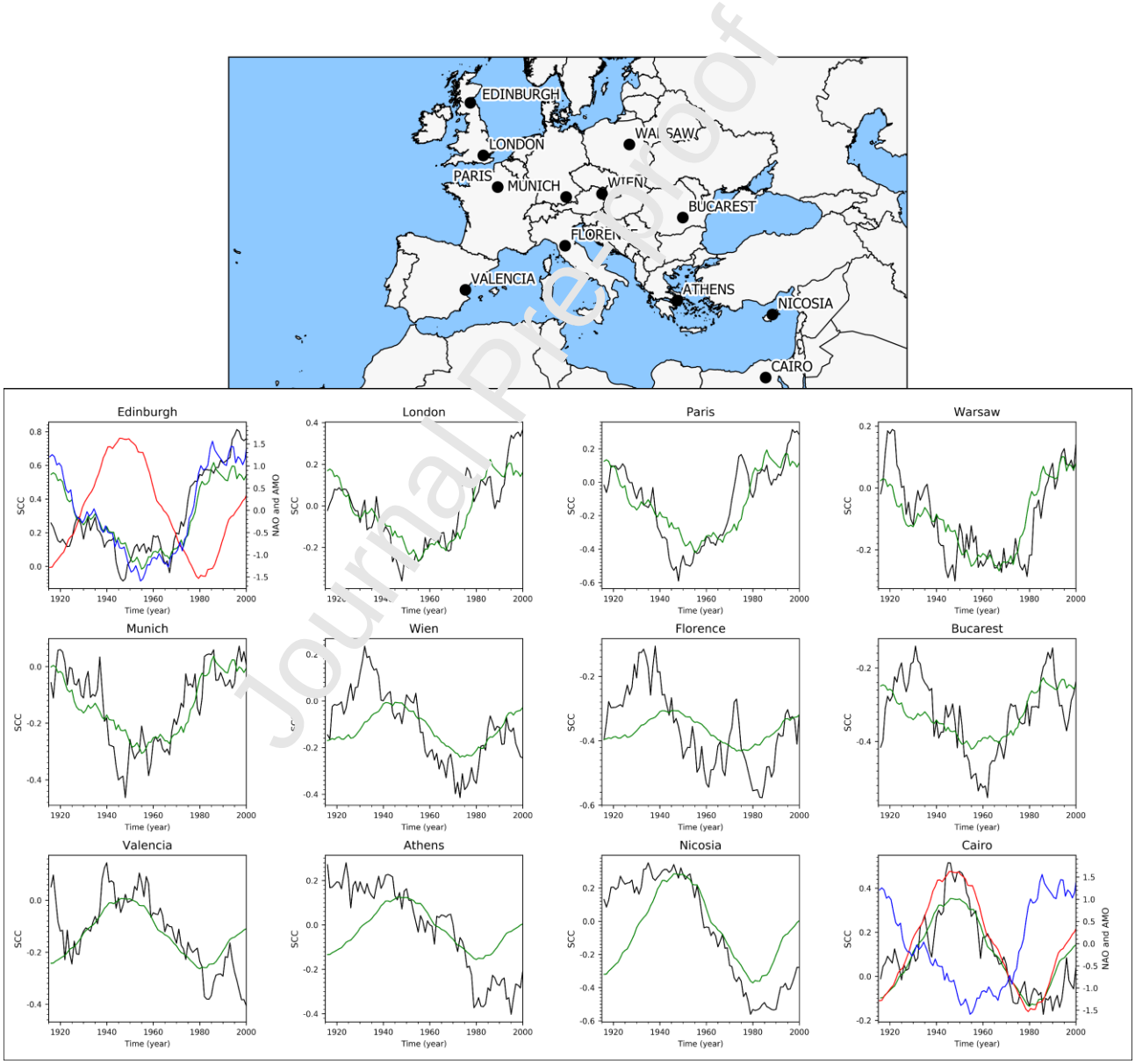

Figure 12: Spearman's correlation coefficient (SCC) between December and March (DJFM) North Atlantic Oscillation (NAO) and DJFM rainfall in different towns of Europe calculated on a 30-year mobile window (black line); DJFM NAO dataset averaged on a 30-year mobile window (blue line); DJFM Atlantic Multidecadal Oscillation (AMO) averaged on a 30-year mobile window (red line); best-fit curve of the linear model (green line). The model is obtained adding a constant to a linear combination of DJFM NAO and DJFM AMO curves (only non-negative coefficients are allowed).

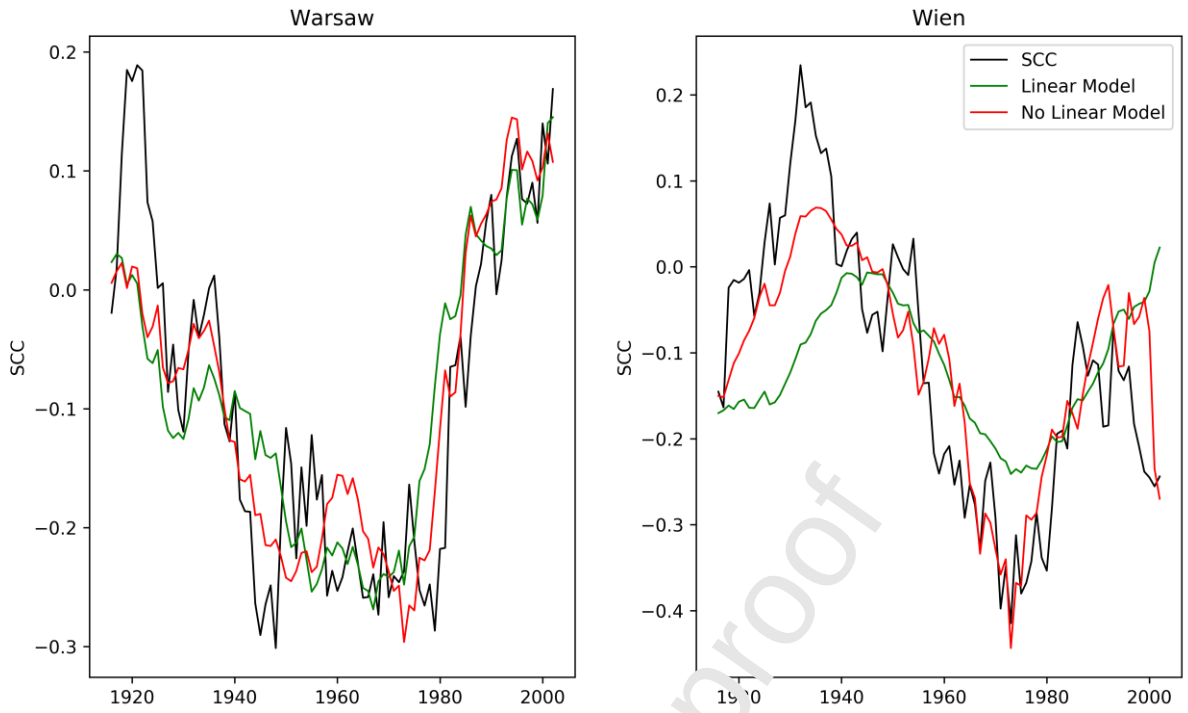

Figure 13: Comparison of the fit of SCC calculated by linear model and non-linear model for Warsaw and Wien. The black and green lines represent the SCC curve and linear model, respectively, as in Figure 12. The red line represents the fit of the SCC curve with a non-linear model

4. Conclusions

The goal of this study was to improve our knowledge of rainfall variability, related in particular to the winter months, and to NAO in Tuscany. Identification of a statistical method able to quantify the correlation among global climatic patterns, North Atlantic Oscillation, and local meteorological patterns, made it possible to describe climatic dependency during the year and over time, considering a rich rainfall historical series from 1920 to date. Our results show an alternation of months with a negative (winter) and positive (summer) correlation. Great spatial variability linked to the two passages of the polar front can be recognized in spring and in autumn, quite remarkable between October and December. Over time, we have observed a decrease in the correlation between NAO and rainfall in Tuscany in the December to-March period between 1960 and 1990. Variations in the DJFM NAO correlation and in DJFM rainfall seem to be linked to DJFM Multidecadal Atlantic Oscillation (AMO), the temperature of the Atlantic surface. Therefore, we built a linear regression model, which allowed us to quantify the role of DJFM AMO in the trend of the correlation coefficient. Extending the study to Northern Europe and to the Mediterranean basin, we observed that the trend of the SCC curve from December to March is regulated by various climatic factors whose variations depend on latitude. In Northern Europe, the NAO index mainly regulates the trend of SCC, while in the southern Mediterranean basin this trend is mainly regulated by the AMO index. In particular, rainfall in Northern Europe (e.g. Great Britain, Northern France, Poland) is associated with the pressure differences between high and low latitudes. On the contrary, in the Mediterranean and especially in the south-eastern zone, rainfall is associated with the cyclical temperature of the Atlantic Ocean. Moving from high to low latitudes, we noticed a progressive change of regulation and a double regulation dependence in two different physical parameters with different cyclicity.

Consequently, the circulation of moist air masses from the Atlantic Ocean depends on different regulatory factors. The circulation of moist air masses in Northern Europe is linked to the baric differences between high and low latitudes

(represented by the NAO index): indeed, in periods in which the baric depression at low latitudes is very intense, there is a greater amount of perturbation coming from the Atlantic compared to periods in which the baric depression is more limited at high latitudes (Osborn, 2006; Trigo et al., 2004). In the case of the Mediterranean, the SCC curve is linked to sea temperature and this could be associated with higher energy availability; a greater number of Atlantic disruptions can develop at medium latitudes (higher temperature), targeting the Mediterranean and North Africa.

This methodology proved to be valid in investigating the role of global climatic patterns on local effects, making it possible to extend the study to other areas. Further studies using more detailed data, as in the case study of Tuscany, will be able to highlight the trend of the SCC curve so that the linear model can be refined and errors reduced by a more accurate estimate of the curve.

Funding: This research was funded by the Fondazione Cassa di Risparmio di Lucca ("Call 2018") within the project "Cambiamenti globali e impatti locali: conoscenza e consapevolezza per uno sviluppo sostenibile della pianura Apuo-versiliese" (Rp. M. Bini), and by the "Autorità di Bacino Distrettuale Appennino Settentrionale " (collaborative research agreement n. 579999-2019 Rps. M. Bini, R. Giannecchini)

Conflicts of Interest: The authors declare no conflict of interest. The funders had no role in the design of the study; in the collection, analyses, or interpretation of data; in the writing of the manuscript, or in the decision to publish the results.

References

Allan, R.P., 2011. Human influence on rainfall. Nature 470, 344–345. https://doi.org/10.1038/470344a

Barnston, A.G., Livezey, R.E., 1987. Classification, Seasonality and Persistence of Low-Frequency Atmospheric Circulation Patterns. Mon. Weather Rev. 115, 1083–1126. https://doi.org/10.1175/1520-0493(1987)115<1083:CSAPOL>2.0.CO;2

Bates, B., Kundzewicz, Z.W., Wu, S., Burkett, V., Doell, P., Gwary, D., Hanson, C., Heij, B., Jiménez, B., Kaser, G., Kitoh, A., Kovats, S., Kumar, P., Magadza, C.H.D., Martino, D., Mata, L., Medany, M., Miller, K., Arnell, N., 2008. Climate Change and Water. Technical Paper of the Intergovernmental Panel on Climate Change.

Bishara, A.J., Hittner, J.B., 2015. Reducing Bias and Error in the Correlation Coefficient Due to Nonnormality. Educ. Psychol. Meas. 75, 785–804. https://doi.org/10.1177/0013164414557639

Bowley, A.L., 1928. The Standard Deviation of the Correlation Coefficient. J. Am. Stat. Assoc. 23, 31–34. https://doi.org/10.2307/2277400

Brandimarte, L., Di Baldassarre, G., Bruni, G., D'Odorico, P., Montanari, A., D'Odorico, P., Montanari, A., 2011. Relation Between the North-Atlantic Oscillation and Hydroclimatic Conditions in Mediterranean Areas. Water Resour. Manag. 25, 1269–1279. https://doi.org/10.1007/s11269-010-9742-5

Caloiero, T., Coscarelli, R., Ferrari, E., Mancini, M., 2011. Precipitation change in Southern Italy linked to global scale oscillation indexes. Nat. Hazards Earth Syst. Sci. 11, 1683–1694. https://doi.org/10.5194/nhess-11-1683-2011

D'Amato Avanzi, G., Giannecchini, R., Puccinelli, A., 2004. The influence of the geological and geomorphological settings on shallow landslides. An example in a temperate climate environment: the June 19, 1996 event in northwestern Tuscany (Italy). Eng. Geol. 73, 215–228. https://doi.org/https://doi.org/10.1016/j.enggeo.2004.01.005

Dickey, D., Fuller, W., 1979. Distribution of the Estimators for Autoregressive Time Series With a Unit Root. JASA. J.

Am. Stat. Assoc. 74. https://doi.org/10.2307/2286348

European Environment Agency, 2019. Economic losses from climate -related extremes in Europe [WWW Document]. Indic. Assess. URL https://www.eea.europa.eu/data-and-maps/indicators/direct-losses-from-weather-disasters-3/assessment-2 (accessed 1.31.20).

Faust, J.C., Fabian, K., Milzer, G., Giraudeau, J., Knies, J., 2016. Norwegian fjord sediments reveal NAO related winter temperature and precipitation changes of the past 2800 years. Earth Planet. Sci. Lett. 435, 84–93. https://doi.org/https://doi.org/10.1016/j.epsl.2015.12.003

Ferrari, E., Caloiero, T., Coscarelli, R., 2013. Influence of the North Atlantic Oscillation on winter rainfall in Calabria (southern Italy). Theor. Appl. Climatol. 114, 479–494. https://doi.org/10.1007/s00704-013-0856-6

Folland, C.K., Palmer, T.N., Parker, D.E., 1986. Sahel rainfall and worldwide sea temperatures, 1901–85. Nature 320, 602–607. https://doi.org/10.1038/320602a0

Geiger, R., Aron, R.H., Todhunter, P., 1995. The Influence of Topography on the Microclimate BT - The Climate Near the Ground, in: Geiger, R., Aron, R.H., Todhunter, P. (Eds.), . Vieweg+Teubner Verlag, Wiesbaden, pp. 327–406. https://doi.org/10.1007/978-3-322-86582-3_8

Giannecchini, R., 2006. Relationship between rainfall and shallow landslides in the southern Apuan Alps (Italy). Nat. Hazards Earth Syst. Sci. 6, 357–364. https://doi.org/10.5194/nhess-6-357-2006

Giannecchini, R., D'Amato Avanzi, G., 2012. Historical research as a tool in estimating hydrogeological hazard in a typical small alpine-like area: The example of the Versilia River basin (Apuan Alps, Italy). Phys. Chem. Earth, Parts A/B/C 49, 32–43. https://doi.org/10.1016/J.PCE.2011.12.005

Goodess, C.M., Jones, P.D., 2002. Links between circulation and changes in the characteristics of Iberian rainfall. Int. J. Climatol. A J. R. Meteorol. Soc. 22, 1593–1615.

Herrera, R.G., Puyol, D.G., Martín, E.H., Gimeno Presa, L., Rodríguez, P.R., Presa, L.G., Rodríguez, P.R., 2001. Influence of the North Atlantic Oscillation on the Canary Islands Precipitation. J. Clim. 14, 3889–3903. https://doi.org/10.1175/1520-0442(2001)014<3889:IOTNAO>2.0.CO;2

Hurrell, J., National Center for Atmospheric Research Staff, 2020. "The Climate Data Guide: Hurrell North Atlantic Oscillation (NAO) Index (station-based)." [WWW Document]. Clim. Data Guid. URL https://climatedataguide.ucar.edu/climate-data/hurrell-north-atlantic-oscillation-nao-index-station-based. (accessed 2.17.20).

Hurrell, J.W., 1996. Influence of variations in extratropical wintertime teleconnections on northern hemisphere temperature. Geophys. Res. Lett. 23, 665–668. https://doi.org/10.1029/96GL00459

Hurrell, J.W., 1995a. Decadal Trends in the North Atlantic Oscillation: Regional Temperatures and Precipitation. Science (80-.). 269, 676 LP – 679. https://doi.org/10.1126/science.269.5224.676

Hurrell, J.W., 1995b. Transient Eddy Forcing of the Rotational Flow during Northern Winter. J. Atmos. Sci. 52, 2286–2301. https://doi.org/10.1175/1520-0469(1995)052<2286:TEFOTR>2.0.CO;2

Hurrell, J.W., Kushnir, Y., Ottersen, G., Visbeck, M., 2003. An Overview of the North Atlantic Oscillation. North Atl. Oscil. Clim. Significance Environ. Impact, Geophysical Monograph Series. https://doi.org/doi:10.1029/134GM01

Izquierdo, R., Alarcón, M., Aguillaume, L., Àvila, A., 2014. Effects of teleconnection patterns on the atmospheric routes, precipitation and deposition amounts in the north-eastern Iberian Peninsula. Atmos. Environ. 89, 482–490. https://doi.org/https://doi.org/10.1016/j.atmosenv.2014.02.057

J.W. Hurrell, Y. Kushnir, G. Ottersen, M.V. (Eds. ., 2003. The North Atlantic Oscillation: Climatic Significance and Environmental Impact. Geophys. Monogr. Ser. 84, 73. https://doi.org/10.1029/2003eo080005

Kalimeris, A., Ranieri, E., Founda, D., Norrant, C., 2017. Variability modes of precipitation along a Central Mediterranean area and their relations with ENSO, NAO, and other climatic patterns. Atmos. Res. 198, 56–80. https://doi.org/https://doi.org/10.1016/j.atmosres.2017.07.031

Knight, J.R., Allan, R.J., Folland, C.K., Vellinga, M., Mann, M.E., 2005. A signature of persistent natural thermohaline circulation cycles in observed climate. Geophys. Res. Lett. 32. https://doi.org/10.1029/2005GL024233

Knight, J.R., Folland, C.K., Scaife, A.A., 2006. Climate impacts of the Atlantic Multidecadal Oscillation. Geophys. Res. Lett. 33. https://doi.org/10.1029/2006GL026242

Kotsias, G., Lolis, C.J., Hatzianastassiou, N., Levizzani, V., Bartzokas, A., 2020. On the connection between large-scale atmospheric circulation and winter GPCP precipitation over the Mediterranean region for the period 1980-2017. Atmos. Res. 233, 104714. https://doi.org/https://doi.org/10.1016/j.atmosres.2019.104714

Koyama, T., Stroeve, J., 2019. Greenland monthly precipitation analysis from the Arctic System Reanalysis (ASR): 2000–2012. Polar Sci. 19, 1–12. https://doi.org/https://doi.org/10.1016/j.polar.2018.09.001

Lamb, P.J., Peppler, R.A., 1987. North Atlantic Oscillation: Concept and an Application. Bull. Am. Meteorol. Soc. 68, 1218–1225. https://doi.org/10.1175/1520-0477(1987)068<1218:NAOCAA>2.0.CO;2

López-Moreno, J.I., Vicente-Serrano, S.M., Morán-Tejeda, E., Lorenzo-Lacruz, J., Kenawy, A., Beniston, M., 2011. Effects of the North Atlantic Oscillation (NAO) on combined temperature and precipitation winter modes in the Mediterranean mountains: Observed relationships and projections for the 21st century. Glob. Planet. Change 77, 62–76. https://doi.org/https://doi.org/10.1016/j.gloplacha.2011.03.003

Luo, D., Chen, X., Feldstein, S.B., 2018. Linear and Nonlinear Dynamics of North Atlantic Oscillations: A New Thinking of Symmetry Breaking. J. Atmos. Sci. 75, 1955–1977. https://doi.org/10.1175/JAS-D-17-0274.1

Molinari, R.L., Mayer, D.A., Festa, J.F., Bezdek, H.F., 1997. Multiyear variability in the near-surface temperature structure of the midlatitude western North Atlantic Ocean. J. Geophys. Res. Ocean. 102, 3267–3278. https://doi.org/10.1029/96JC03544

Moses, T., Kiladis, G.N., Diaz, H.F., Barry, R.G., 1987. Characteristics and frequency of reversals in mean sea level pressure in the north Atlantic sector and their relationship to long-term temperature trends. J. Climatol. 7, 13–30. https://doi.org/10.1002/joc.3370070104

Muñoz-Díaz, D., Rodrigo, F.S., 2003. Effects of the North Atlantic Oscillation on the probability for climatic categories of local monthly rainfall in southern Spain. Int. J. Climatol. A J. R. Meteorol. Soc. 23, 381–397.

Nalley, D., Adamowski, J., Biswas, A., Gharabaghi, B., Hu, W., 2019. A multiscale and multivariate analysis of precipitation and streamflow variability in relation to ENSO, NAO and PDO. J. Hydrol. 574, 288–307. https://doi.org/https://doi.org/10.1016/j.jhydrol.2019.04.024

Osborn, T.J., 2006. Recent variations in the winter North Atlantic Oscillation. Weather 61, 353–355. https://doi.org/10.1256/wea.190.06

Parker, D.E., Folland, C.K., 1988. The nature of climatic variability. Meteorol. Mag. 117, 201–210.

Qian, C., Zhou, W., Fong, S.K., Leong, K.C., 2015. Two approaches for statistical prediction of non-gaussian climate extremes: A case study of macao hot extremes during 1912-2012. J. Clim. 28, 623–636. https://doi.org/10.1175/JCLI-D-14-00159.1

Rapetti, F., Vittorini, S., 1994. Le precipitazioni in Toscana: osservazioni sui casi estremi. Riv. Geogr. Ital. 101, 47–76.

Reverdin, G., Cayan, D., Kushnir, Y., 1997. Decadal variability of hydrography in the upper northern North Atlantic in 1948–1990. J. Geophys. Res. Ocean. 102, 8505–8531. https://doi.org/10.1029/96JC03943

Ríos-Cornejo, D., Penas, Á., Álvarez-Esteban, R., del Río, S., 2015. Links between teleconnection patterns and

precipitation in Spain. Atmos. Res. 156, 14–28.

Rogers, J.C., 1990. Patterns of Low-Frequency Monthly Sea Level Pressure Variability (1899–1986) and Associated Wave Cyclone Frequencies. J. Clim. 3, 1364–1379. https://doi.org/10.1175/1520-0442(1990)003<1364:POLFMS>2.0.CO;2

Romano, E., Preziosi, E., 2013. Precipitation pattern analysis in the Tiber River basin (central Italy) using standardized indices. Int. J. Climatol. 33, 1781–1792. https://doi.org/10.1002/joc.3549

Rousi, E., Rust, H.W., Ulbrich, U., Anagnostopoulou, C., 2020. Implications of Winter NAO Flavors on Present and Future European Climate. Climate 8, 13. https://doi.org/10.3390/cli8010013

Spearman, C., 1904. The proof and measurement of association between two things. Am. J. Psychol. 15, 72–101. https://doi.org/10.2307/1412159

Stagl, J., Mayr, E., Koch, H., Hattermann, F.F., Huang, S., 2014. Effects of Climate Change on the Hydrological Cycle in Central and Eastern Europe BT - Managing Protected Areas in Central and Eastern Europe Under Climate Change, in: Rannow, S., Neubert, M. (Eds.), . Springer Netherlands, Dordrecht, pp. 31–43.

Trigo, R.M., Pozo-Vázquez, D., Osborn, T.J., Castro-Díez, Y., Gámiz-Fortis, S., Esteban-Parra, M.J., Pozo-Vázquez, D., Osborn, T.J., Castro-Díez, Y., Gámiz-Fortis, S., Esteban-Parra, M.J., 2004. North Atlantic Oscillation influence on precipitation, river flow and water resources in the Iberian Peninsula. Int. J. Climatol. A J. R. Meteorol. Soc. 24, 925–944. https://doi.org/10.1002/joc.1048

Ulbrich, U., Christoph, M., Pinto, J.G., Corte-Real, J., 1999. Dependence of winter precipitation over Portugal on NAO and baroclinic wave activity. Int. J. Climatol. 19, 379–390. https://doi.org/10.1002/(SICI)1097-0088(19990330)19:4<379::AID-JOC357>3.0.CO;2-8

van Loon, H., Rogers, J.C., 1978. The Seesaw in Winter Temperatures between Greenland and Northern Europe. Part I: General Description. Mon. Weather Rev. 106, 296–310. https://doi.org/10.1175/1520-0493(1978)106<0296:TSIWTB>2.0.CO;2

Van Loon, H., Williams, J., 1976. The Connection Between Trends of Mean Temperature and Circulation at the Surface: Part I. Winter. Mon. Weather Rev. 104, 365–380. https://doi.org/10.1175/1520-0493(1976)104<0365:TCBTOM>2.0.CO;2

Vergni, L., Di Lena, B., Chiaudani, A., 2016. Statistical characterisation of winter precipitation in the Abruzzo region (Italy) in relation to the North Atlantic Oscillation (NAO). Atmos. Res. 178–179, 279–290. https://doi.org/https://doi.org/10.1016/j.atmosres.2016.03.028

Vicente-Serrano, S.M., López-Moreno, J.I., 2008. Nonstationary influence of the North Atlantic Oscillation on European precipitation. J. Geophys. Res. Atmos. 113. https://doi.org/10.1029/2008JD010382

WMO, 2007. THE ROLE OF CLIMATOLOGICAL NORMALS IN A CHANGING CLIMATE World Climate Data and Monitoring Programme. WCDMP-No. 61.

Xu, H., Taylor, R.G., Xu, Y., 2011. Quantifying uncertainty in the impacts of climate change on river discharge in sub-catchments of the Yangtze and Yellow River Basins, China. Hydrol. Earth Syst. Sci. 15, 333–344. https://doi.org/10.5194/hess-15-333-2011

Zorita, E., Kharin, V., von Storch, H., 1992. The Atmospheric Circulation and Sea Surface Temperature in the North Atlantic Area in Winter: Their Interaction and Relevance for Iberian Precipitation. J. Clim. 5, 1097–1108. https://doi.org/10.1175/1520-0442(1992)005<1097:TACASS>2.0.CO;2

Marco Luppichini: Conceptualization, Methodology, Software, Investigation, Data curation, Writing- Original draft preparation **Michele Barsanti** Conceptualization, Methodology , Software, Investigation, Writing- Original draft preparation. **Roberto Giannecchini**: Supervision, Visualization, Writing- Reviewing and Editing. ***Monica Bini****:* Supervision, Writing- Reviewing and Editing, Conceptualization

Declaration of interests

☒ The authors declare that they have no known competing financial interests or personal relationships that could have appeared to influence the work reported in this paper.

☐The authors declare the following financial interests/personal relationships which may be considered as potential competing interests:

Conflicts of Interest

The authors declare no conflict of interest. The funders had no role in the design of the study; in the collection, analyses, or interpretation of data; in the writing of the manuscript, or in the decision to publish the results.

Highlights

1. Statistical correlation between North Atlantic Oscillation and rainfall
2. Link between global patterns and local-scale effects
3. Variability of correlation over time between NAO and rainfall
4. Role of Atlantic Multidecadal Oscillation on the relationship between NAO and rainfall in Europe.

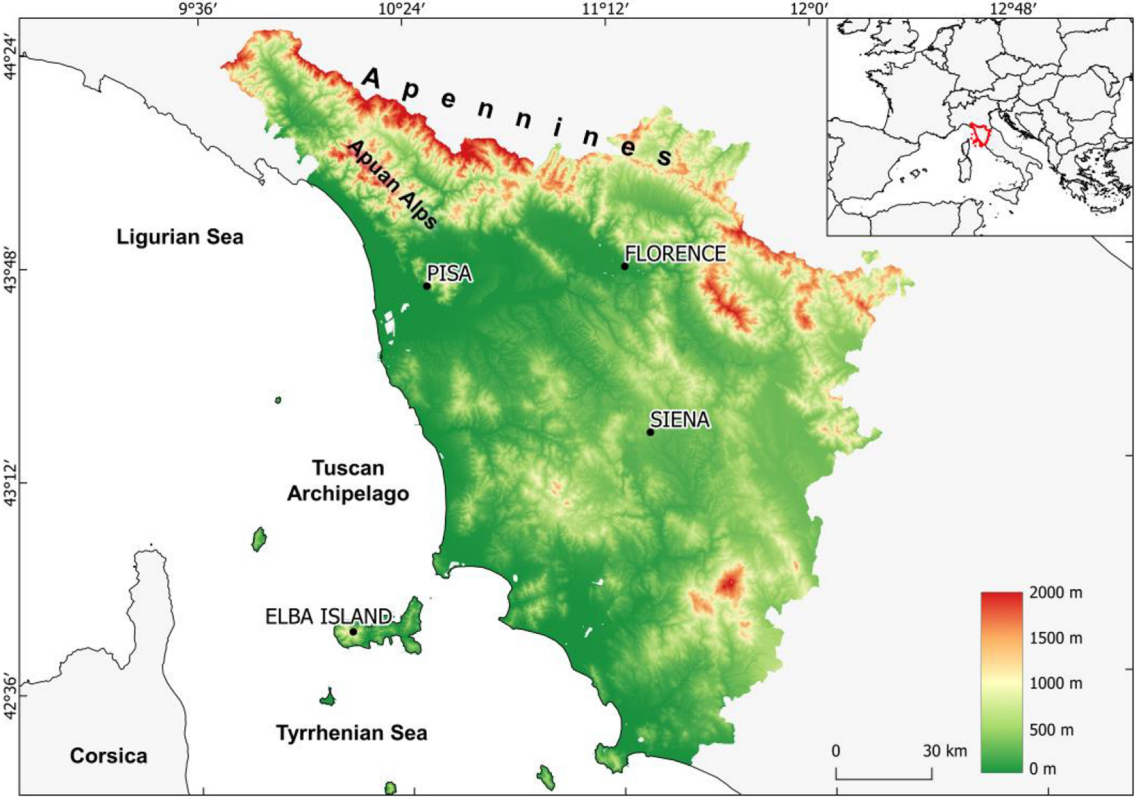
9°36′
10°24′
11°12′
12°0′
12°48′
44°24′
43°48′
43°12′
42°36′
Apennines
Apuan Alps
Ligurian Sea
PISA
FLORENCE
SIENA
Tuscan
Archipelago
ELBA ISLAND
Tyrrhenian Sea
Corsica
2000 m
1500 m
1000 m
500 m
0 m
0
30 km

Figure 1

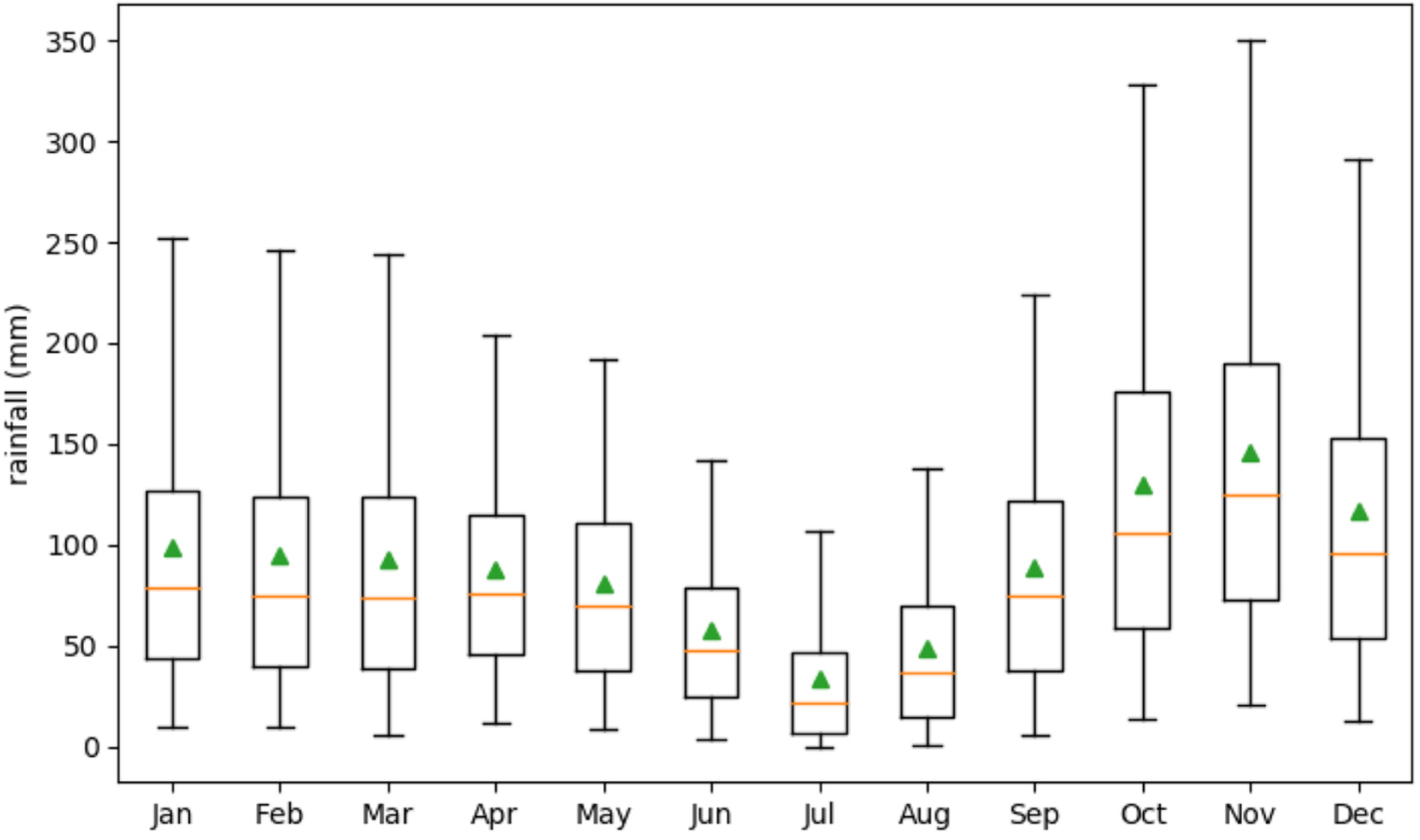
rainfall (mm)
350
300
250
200
150
100
50
0
Jan
Feb
Mar
Apr
May
Jun
Jul
Aug
Sep
Oct
Nov
Dec

Figure 2

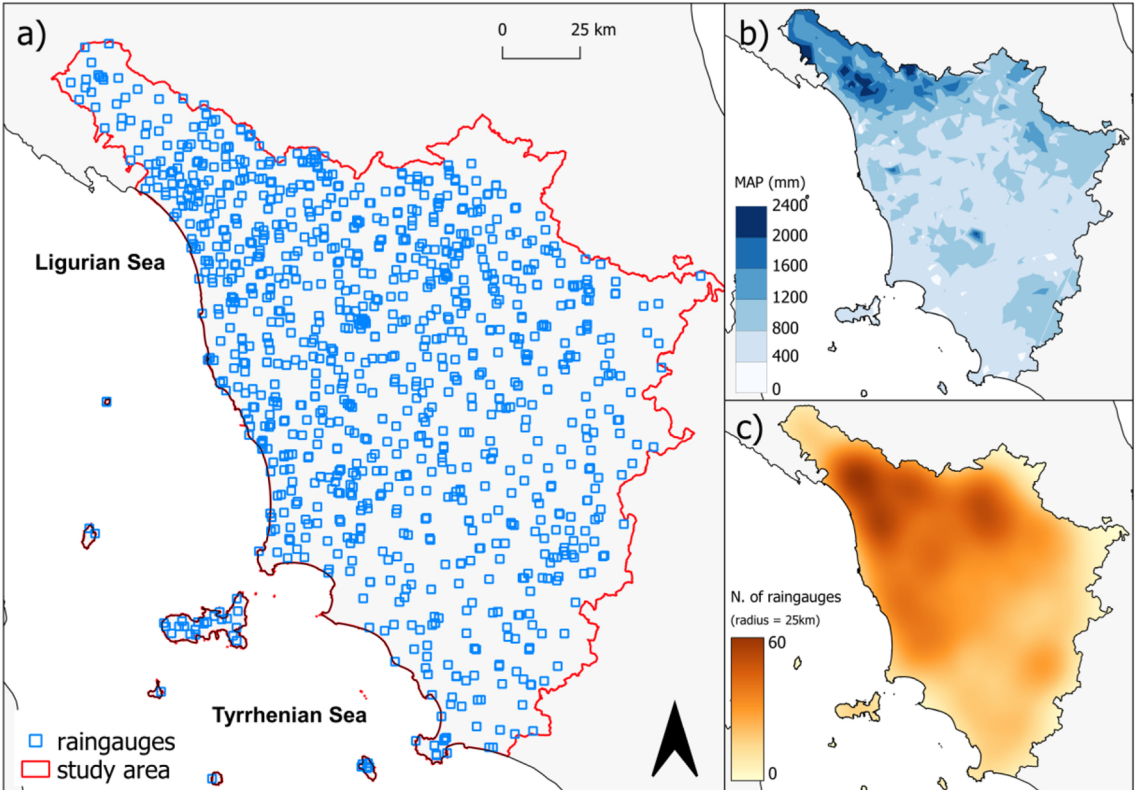
a)
0
25 km
Ligurian Sea
Tyrrhenian Sea
raingauges
study area
b)
MAP (mm)
2400
2000
1600
1200
800
400
0
c)
N. of raingauges
(radius = 25km)
60
0

Figure 3

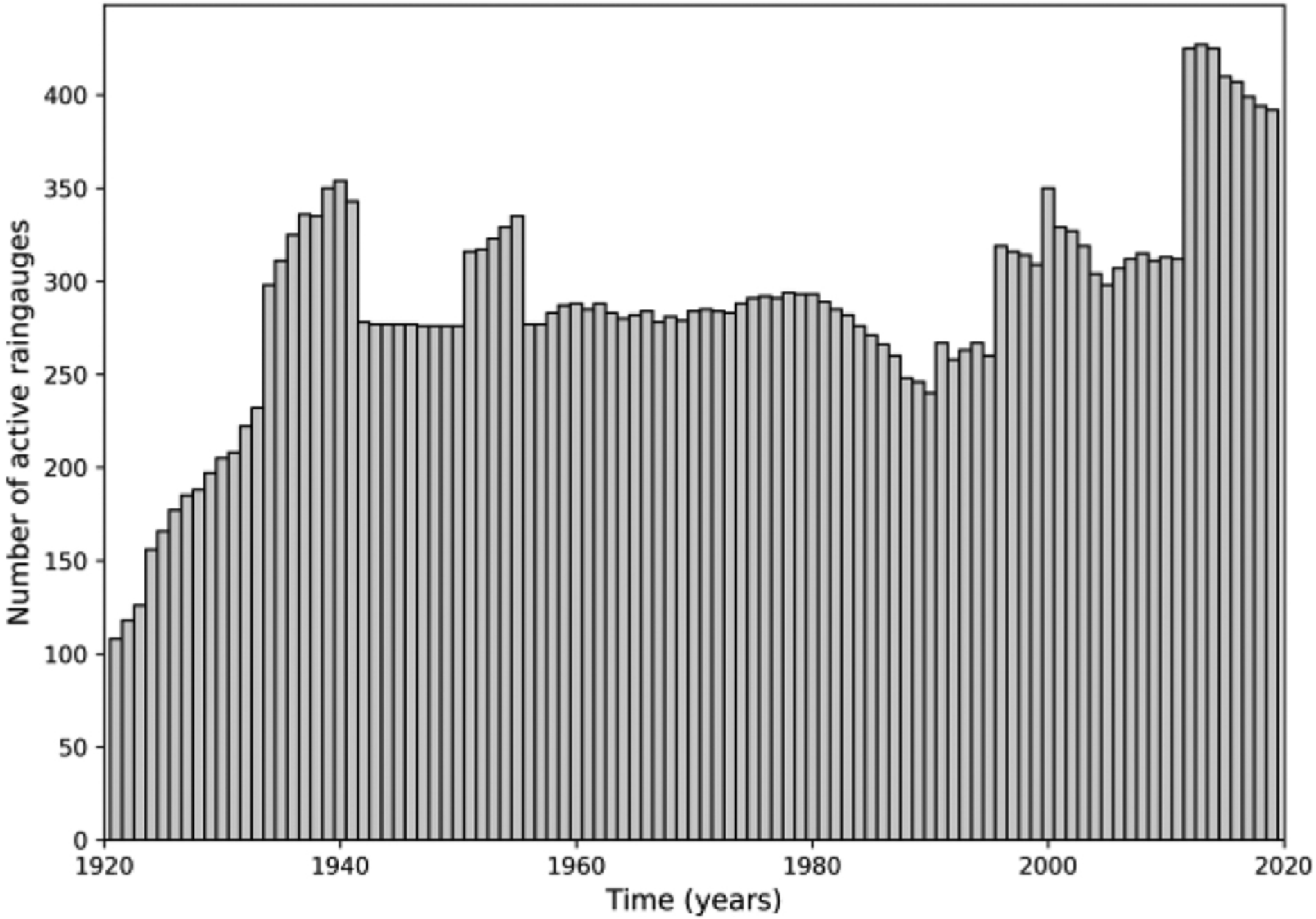
Number of active raingauges
0
50
100
150
200
250
300
350
400
1920
1940
1960
1980
2000
2020
Time (years)

Figure 4

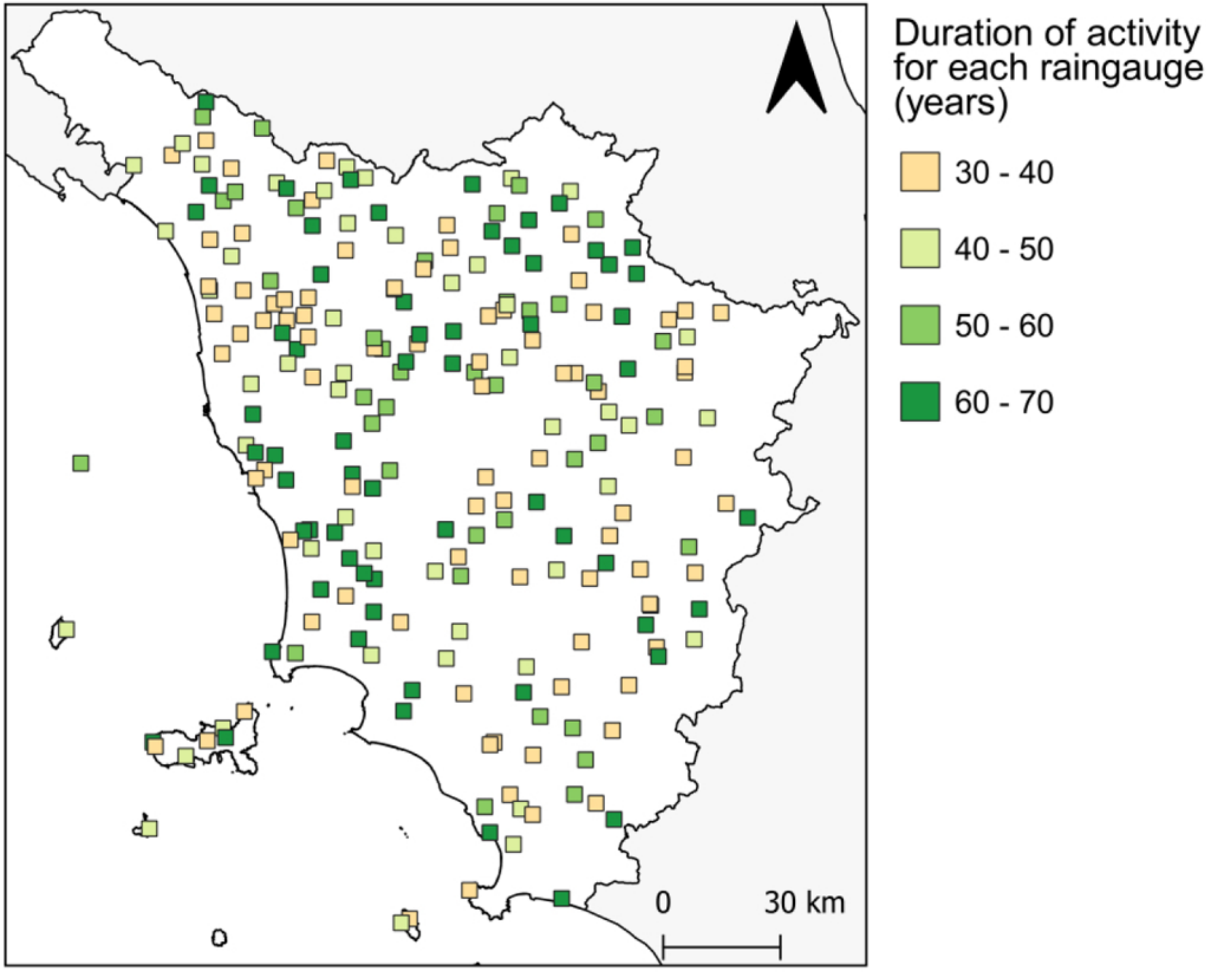
Duration of activity for each raingauge (years)
30 - 40
40 - 50
50 - 60
60 - 70
0
30 km

Figure 5

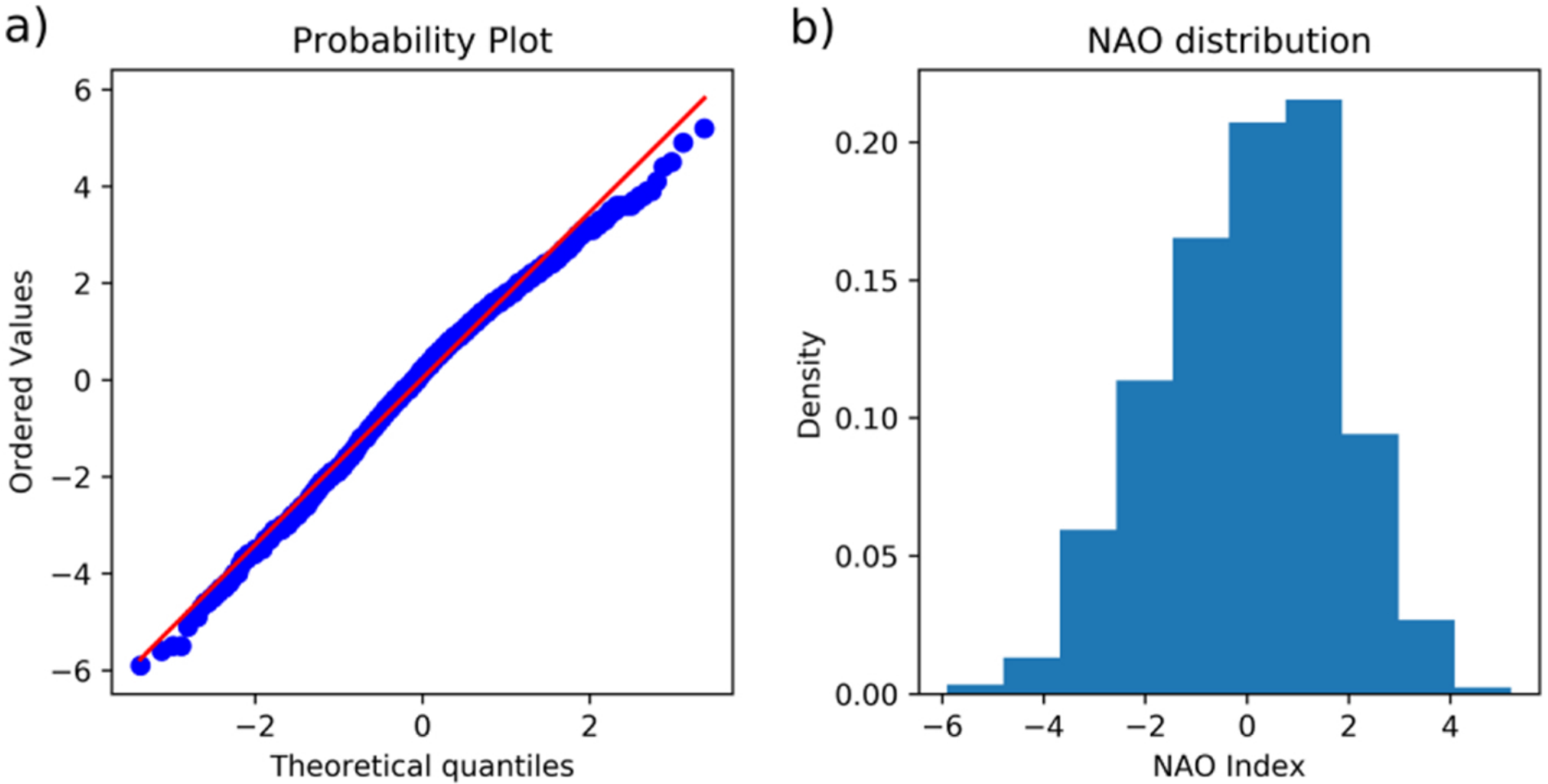
a)
Probability Plot
Ordered Values
Theoretical quantiles
6
4
2
0
−2
−4
−6
−2
0
2
b)
NAO distribution
Density
NAO Index
0.20
0.15
0.10
0.05
0.00
−6
−4
−2
0
2
4

Figure 6

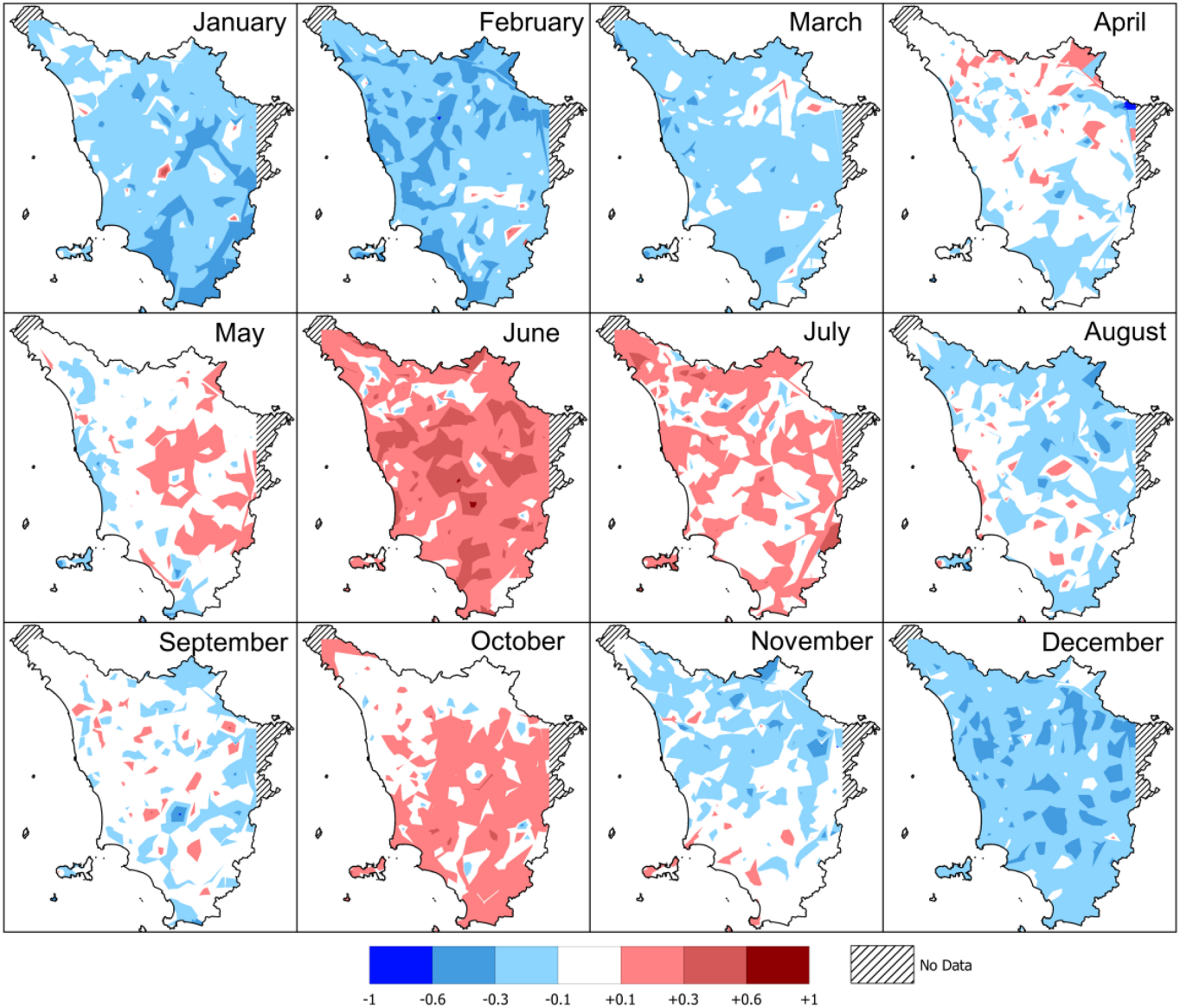
January
February
March
April
May
June
July
August
September
October
November
December
-1
-0.6
-0.3
-0.1
+0.1
+0.3
+0.6
+1
No Data

Figure 7

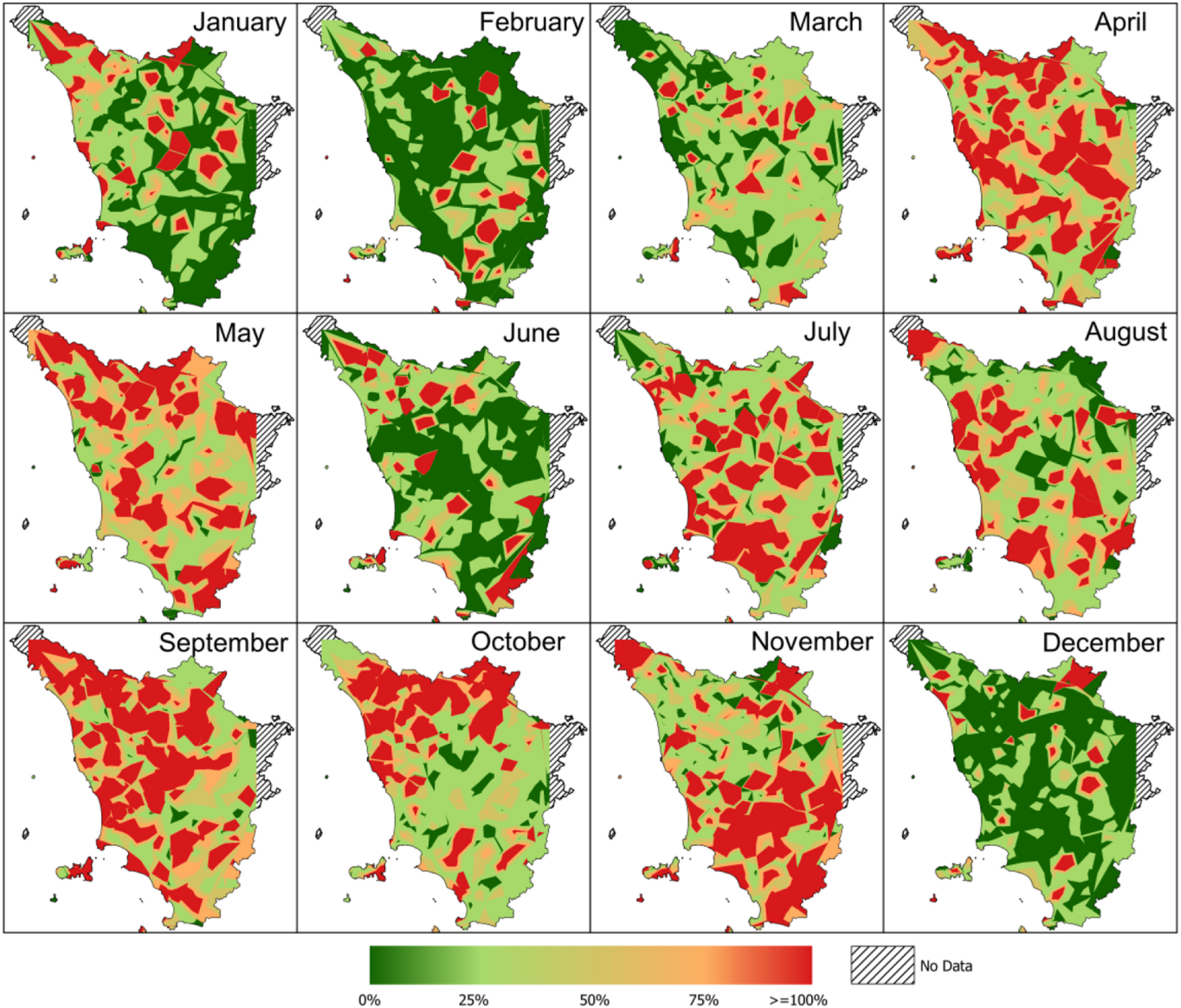
January
February
March
April
May
June
July
August
September
October
November
December
0%
25%
50%
75%
>=100%
No Data

Figure 8

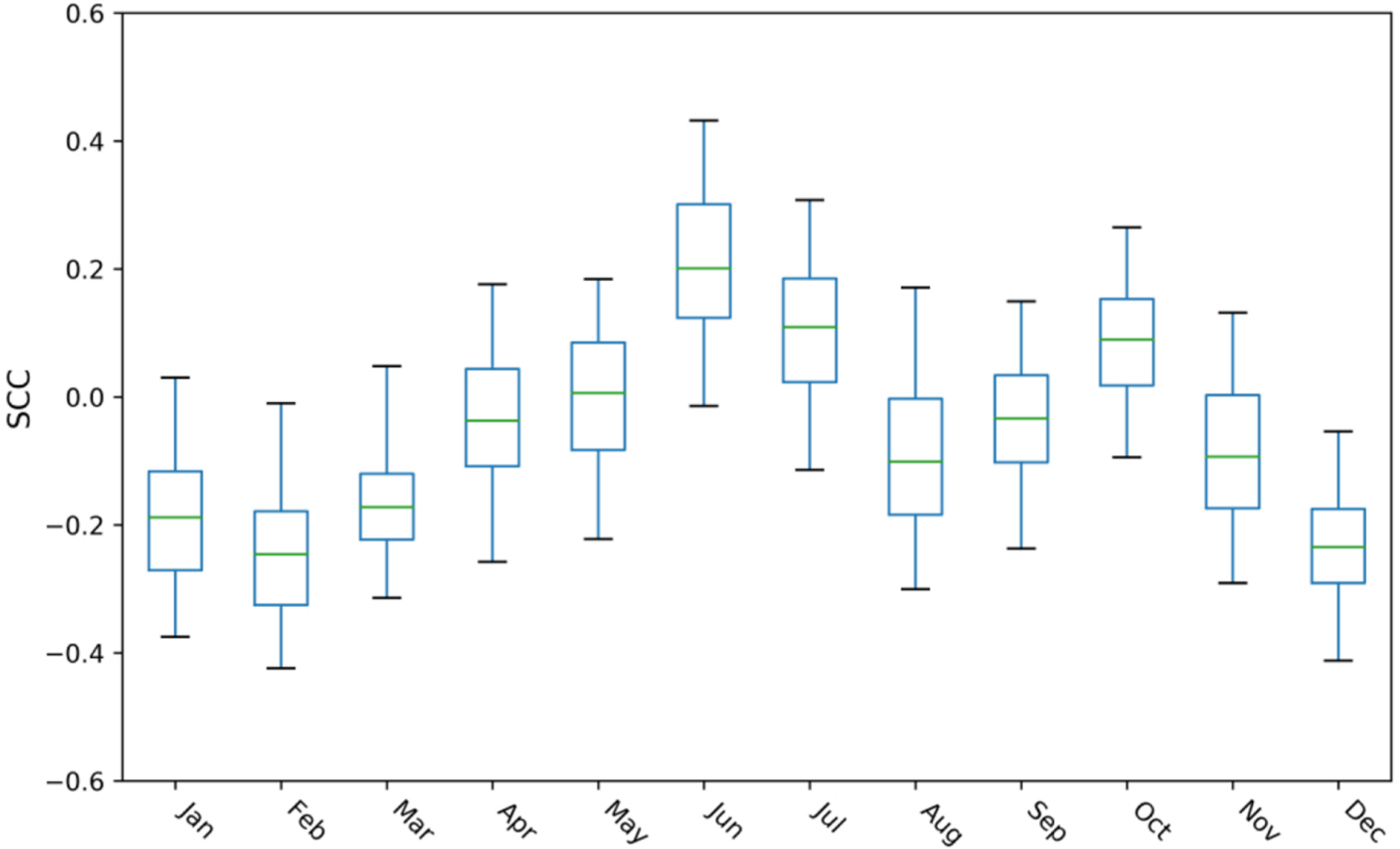
SCC
0.6
0.4
0.2
0.0
−0.2
−0.4
−0.6
Jan
Feb
Mar
Apr
May
Jun
Jul
Aug
Sep
Oct
Nov
Dec

Figure 9

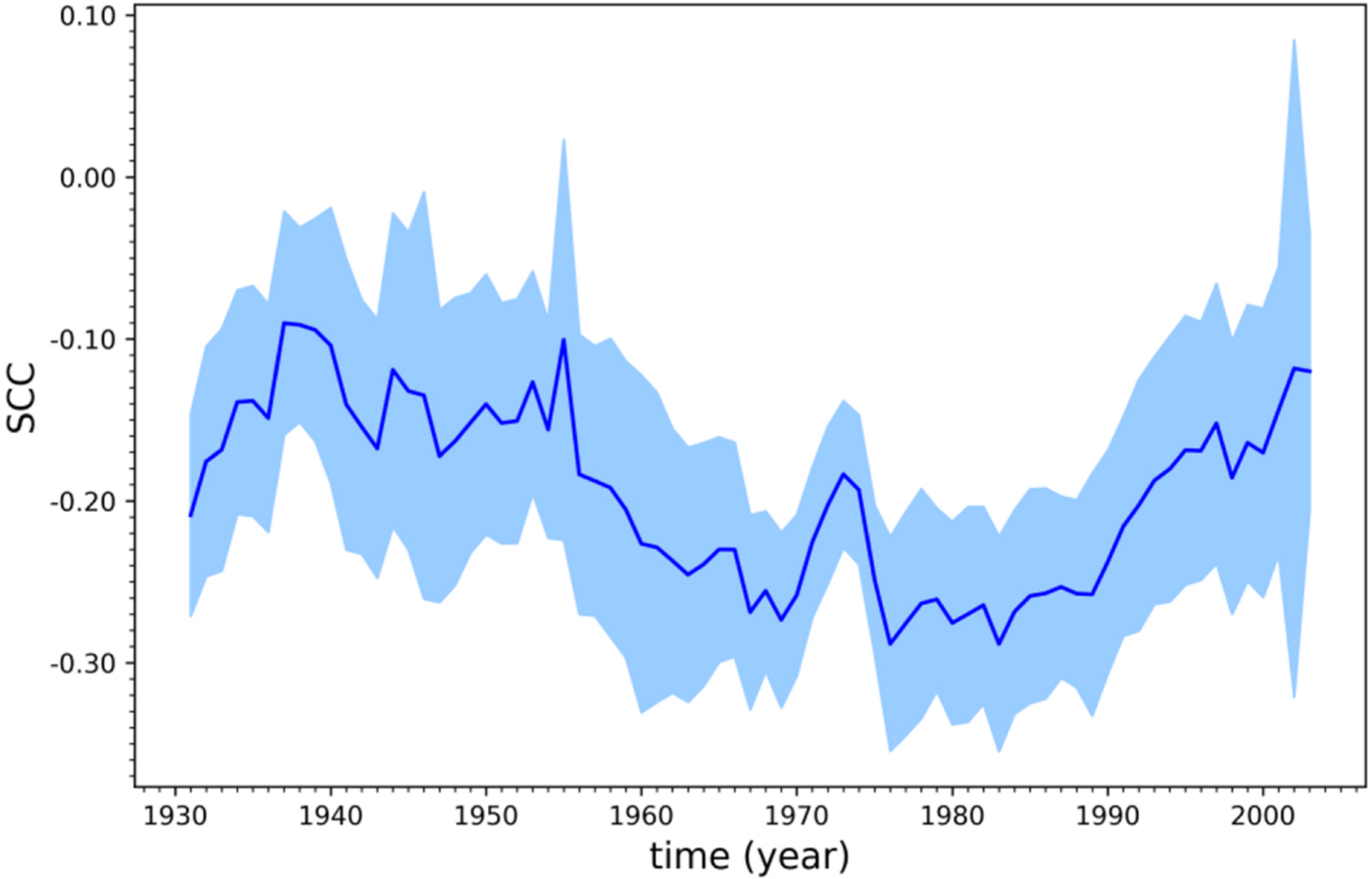
0.10
0.00
-0.10
-0.20
-0.30
SCC
1930
1940
1950
1960
1970
1980
1990
2000
time (year)

Figure 10

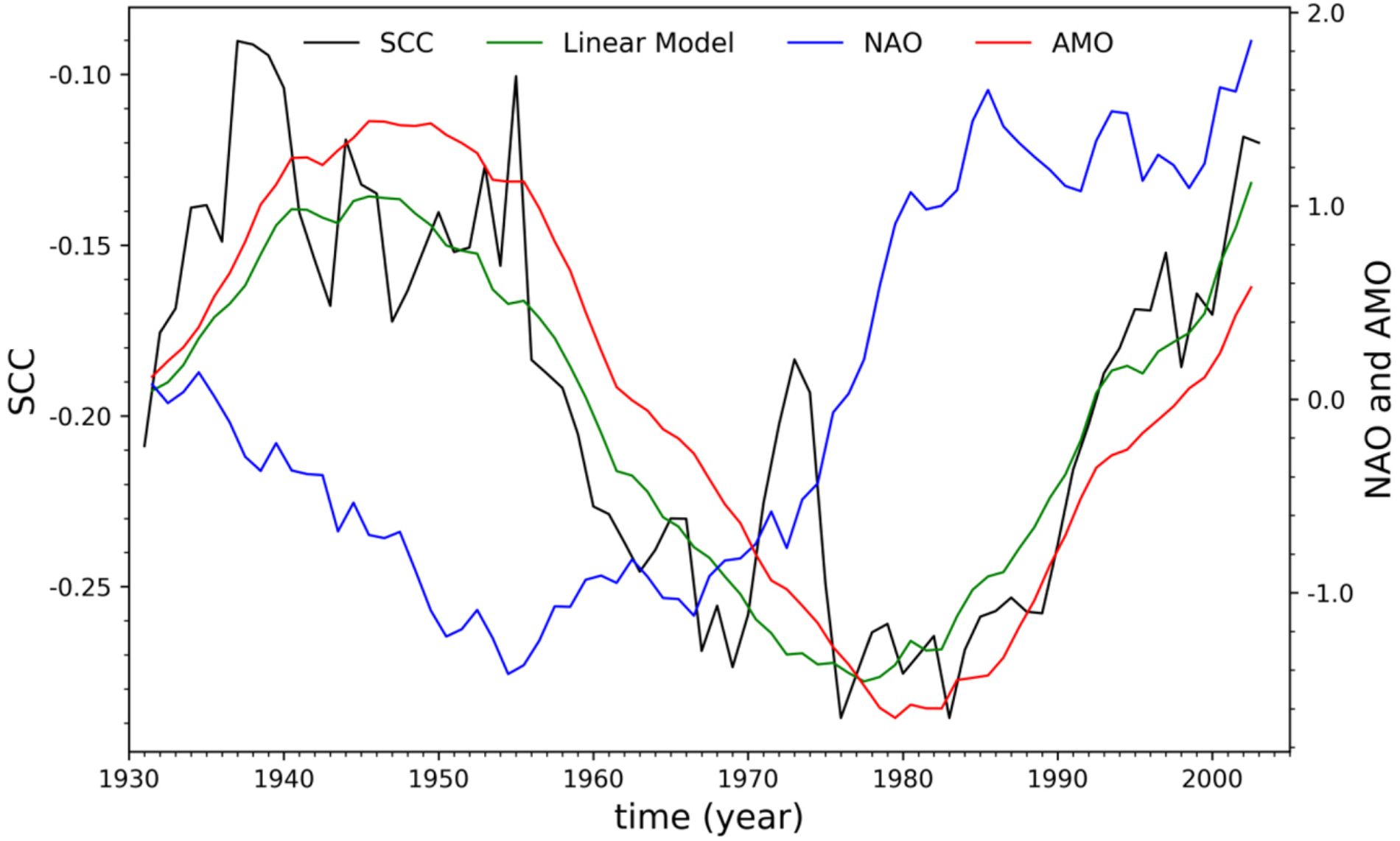
SCC
Linear Model
NAO
AMO
-0.10
-0.15
-0.20
-0.25
SCC
2.0
1.0
0.0
-1.0
NAO and AMO
1930
1940
1950
1960
1970
1980
1990
2000
time (year)

Figure 11

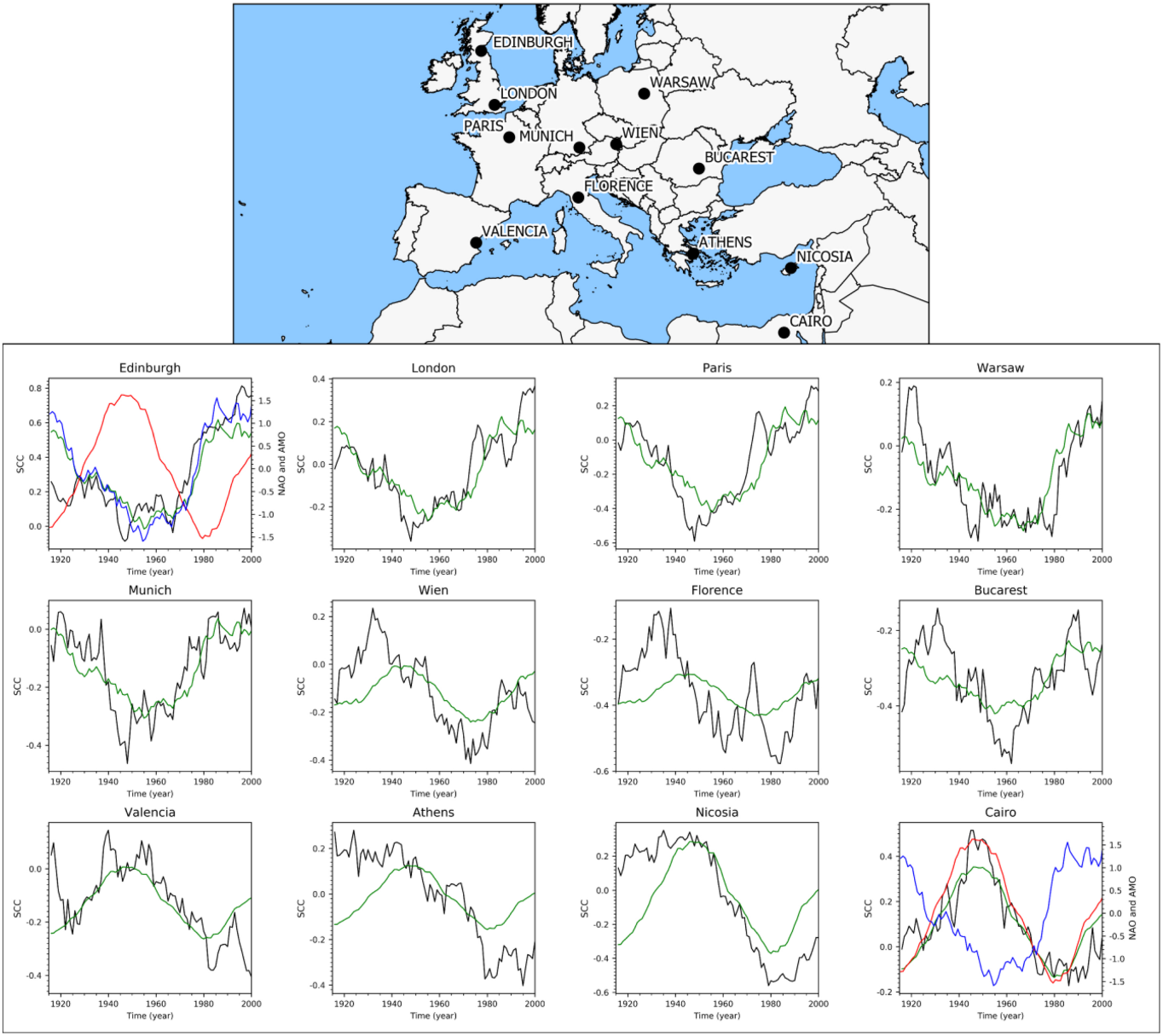
EDINBURGH
LONDON
PARIS
MUNICH
WARSAW
WIEN
BUCAREST
FLORENCE
VALENCIA
ATHENS
NICOSIA
CAIRO
Edinburgh
London
Paris
Warsaw
Munich
Wien
Florence
Bucarest
Valencia
Athens
Nicosia
Cairo
SCC
NAO and AMO
Time (year)

Figure 12

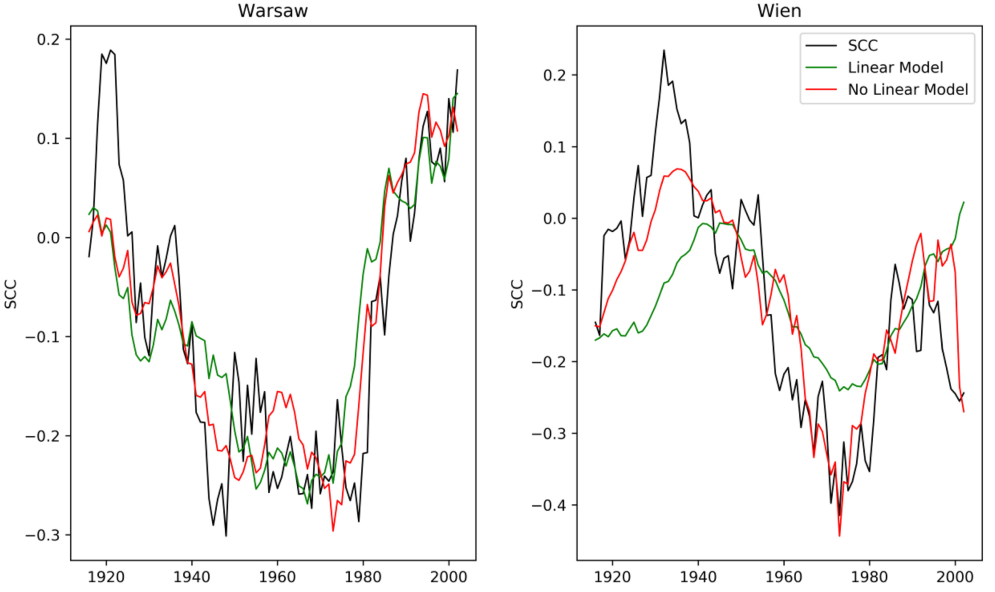
Warsaw
Wien
SCC
Linear Model
No Linear Model
SCC
SCC
0.2
0.1
0.0
−0.1
−0.2
−0.3
−0.4
1920
1940
1960
1980
2000

Figure 13